Observed equatorial waves

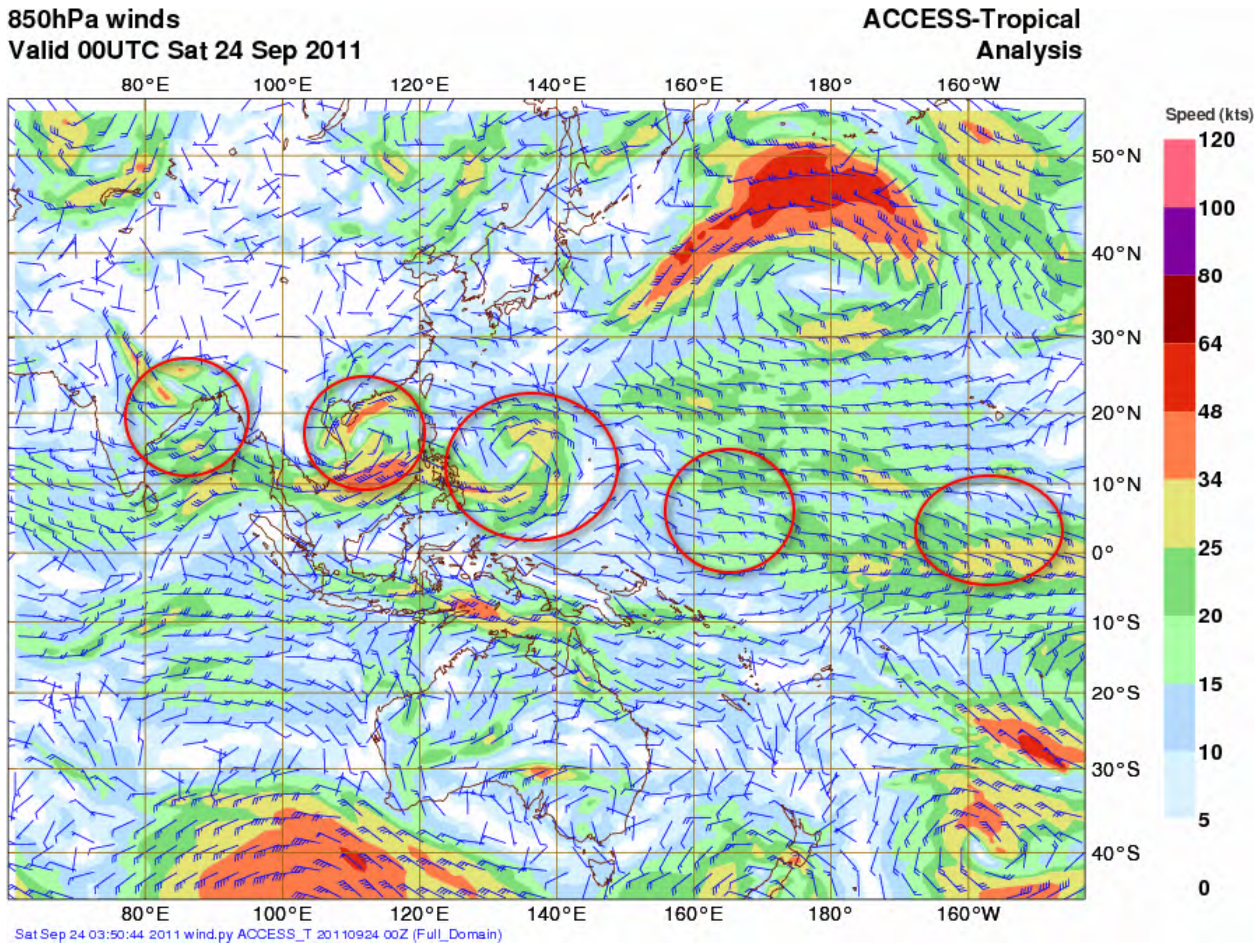

850hPa winds
Valid 00UTC Sat 24 Sep 2011
ACCESS-Tropical
Analysis
80°E
100°E
120°E
140°E
160°E
180°
160°W
50°N
40°N
30°N
20°N
10°N
0°
10°S
20°S
30°S
40°S
Speed (kts)
120
100
80
64
48
34
25
20
15
10
5
0
Sat Sep 24 03:50:44 2011 wind.py ACCESS_T 20110924 00Z (Full_Domain)

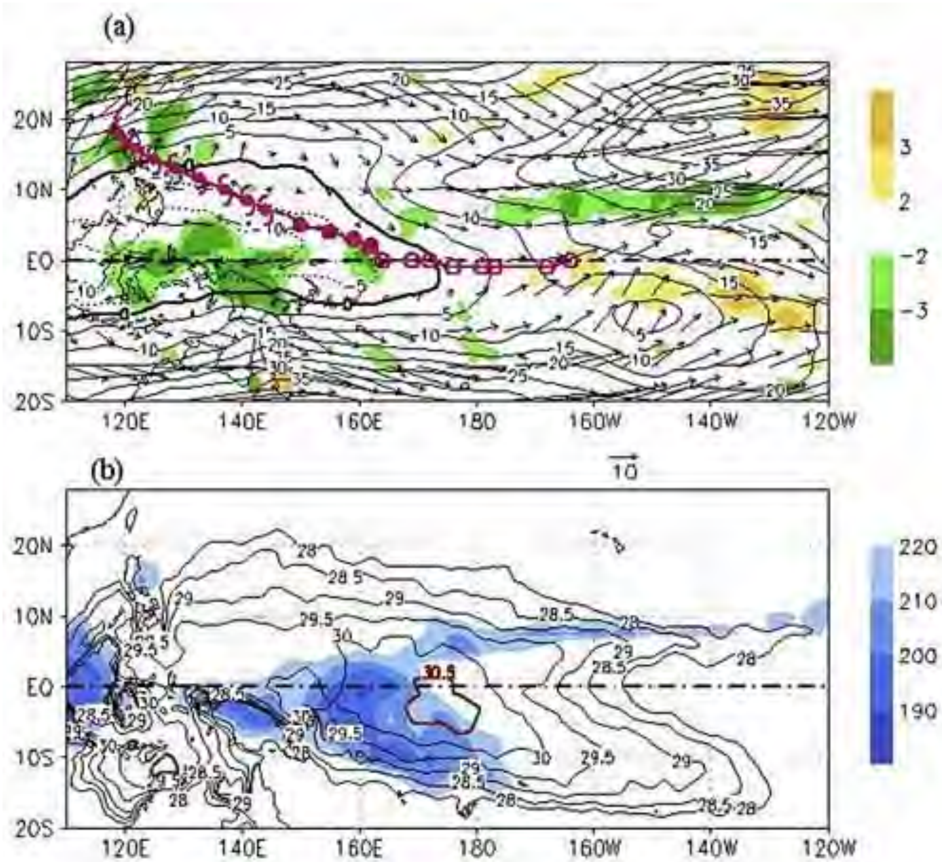

(a) The 11-day (22 Nov. – 2 Dec. 2004) mean amplitude of the vertical shear (200 hPa–850 hPa) of horizontal wind (contour, m/s) and the divergence (⍰ 10⍰ 6 s⍰ 1, shading) at 850 hpa. The line marked with the open circles, closed circles, and typhoon signs represents the movement of typhoon Nanmadol during the period of MRG wave, tropical depression/tropical storm, and typhoon respectively. (b) Time-mean (13 Nov.–12 Dec.) OLR (shading <220 w/m2) and sea surface temperature (°C).

Zhou and Wang (2007): GRL

Transition from an eastern Pacific upper-level mixed Rossby-gravity wave to a western Pacific tropical cyclone

MJO skematic (2_D)

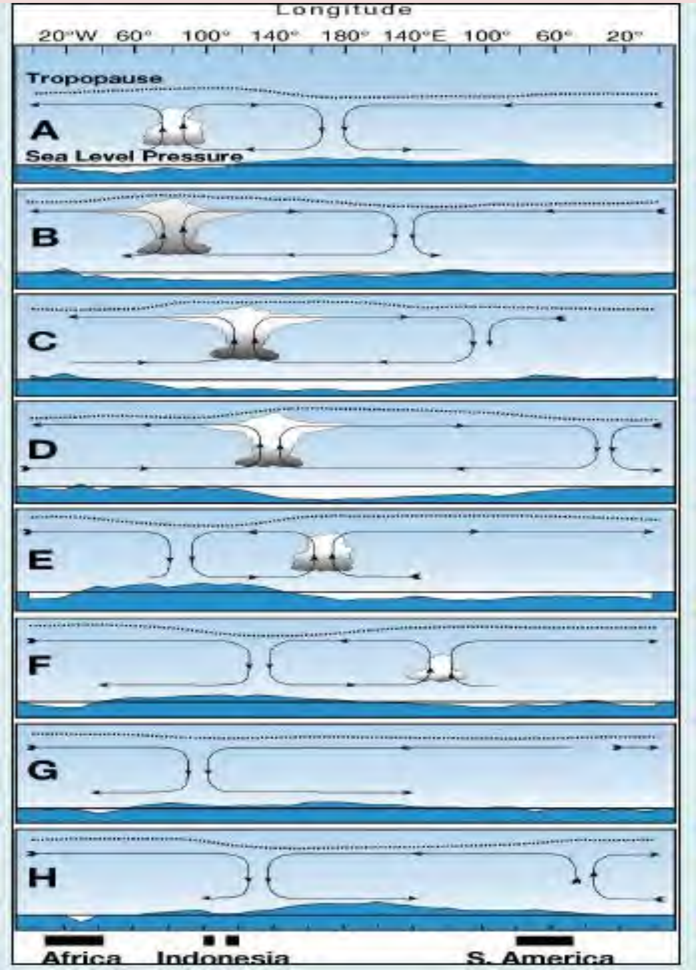

1. Planetary scale zonal circulation coupled with large scale of convective anomalies.
2. Slow eastward propagation gives rise to a 40-50 day spectral peak
3. Development over IO and decay east of dateline
4. Baroclinic structure with Low SLP leading convective anomalies

What about horizontal?

Madden and Julian 1972 , reproduced by McPhaden

Schematic of three-Dimensional MJO Structure

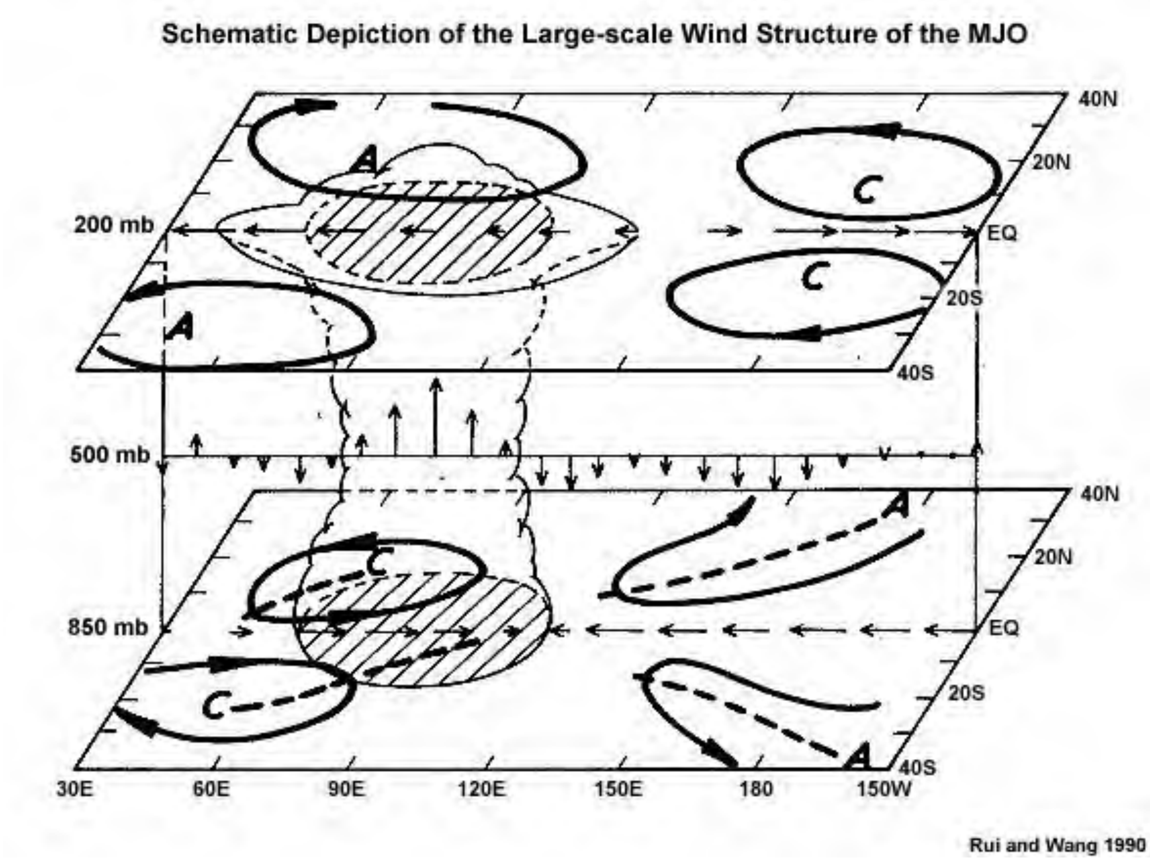

Rui and Wang 1990

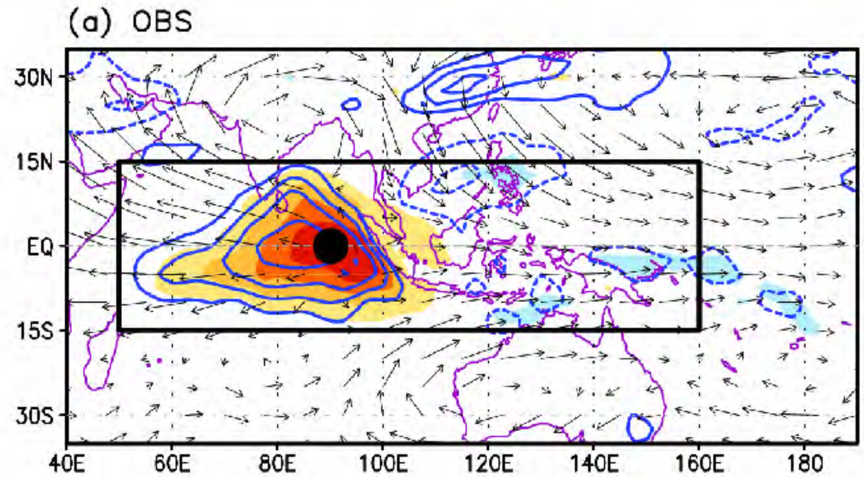

200hPa winds and divergence

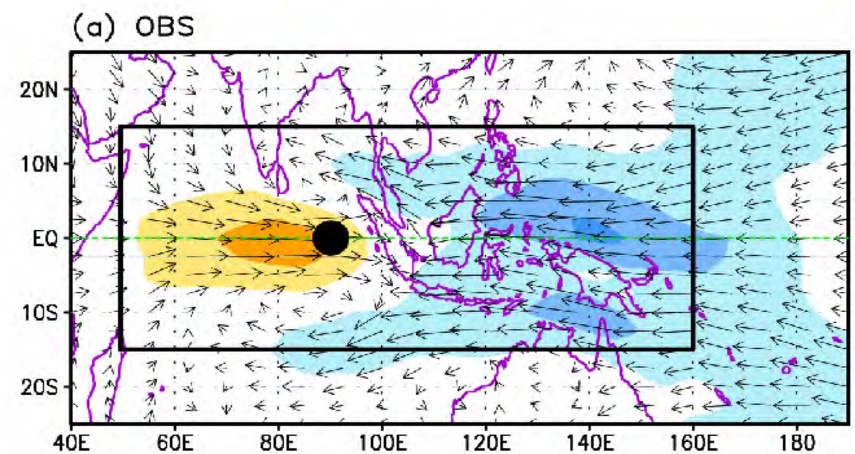

850 hPa winds and u-component

Observed structure of MJO

Wang and Lee 2017

The horizontal and baroclinic structure is a consequence of coupling of convective complex and Kelvin and Rossby waves

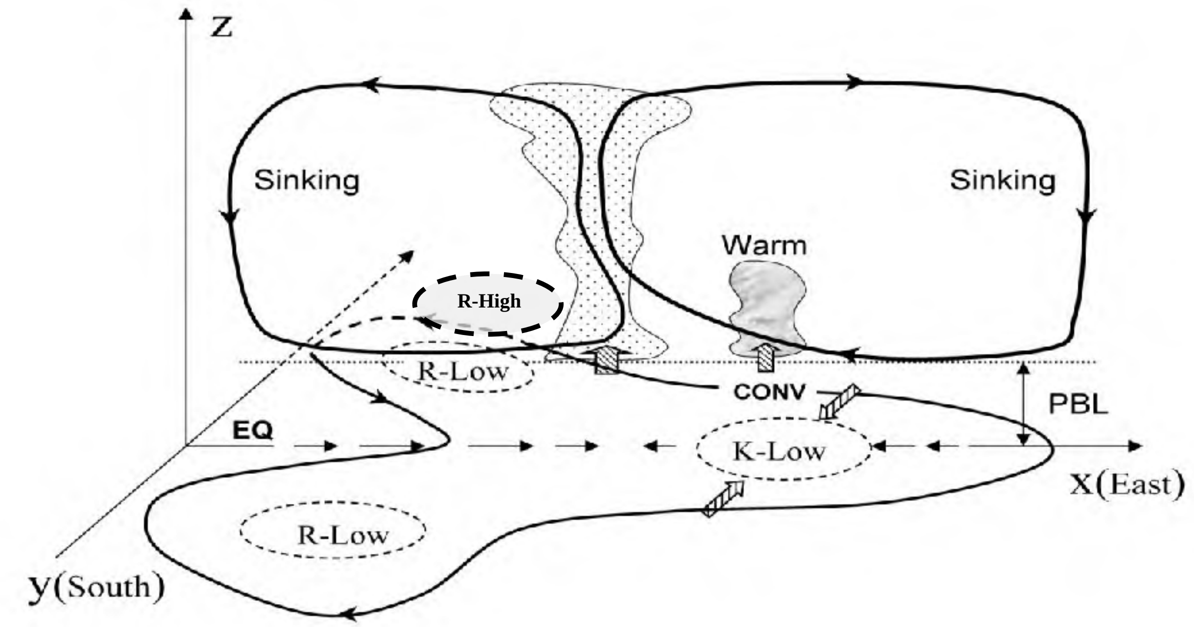

Wang (2005)

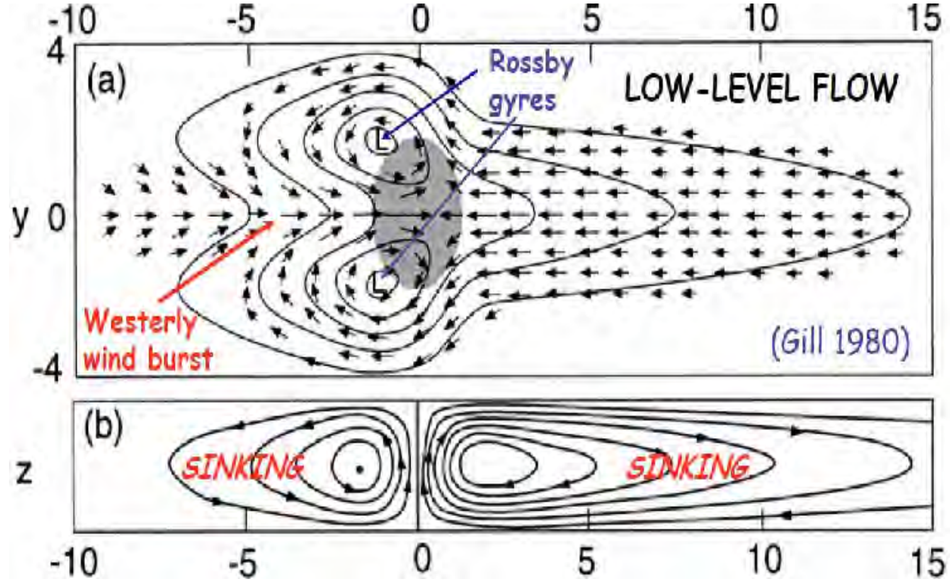
(a)
LOW-LEVEL FLOW
Rossby
gyres
L
L
Westerly
wind burst
(Gill 1980)
y
(b)
z
SINKING
SINKING
-10
-5
0
5
10
15
4
0
-4

Space-time spectra showing the organization of convection in association with theoretical equatorial waves.

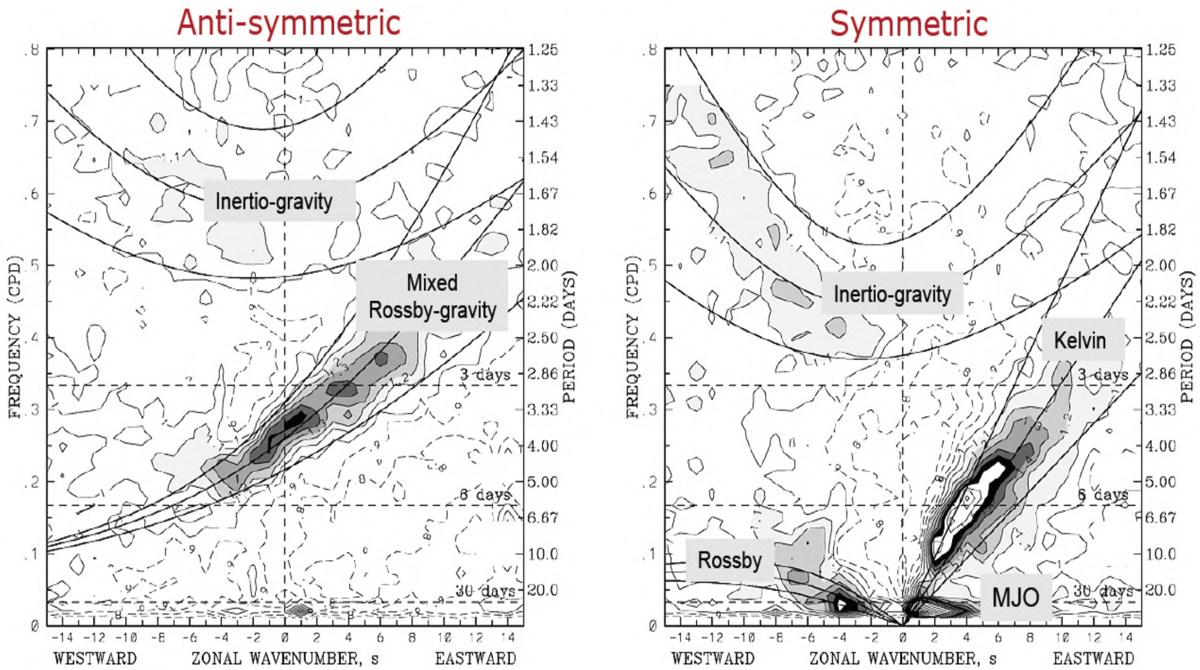

From Wheeler and Kiladis 1999: J. Atmos. Sci.

Observed multi-scale structure of MJO convective complex

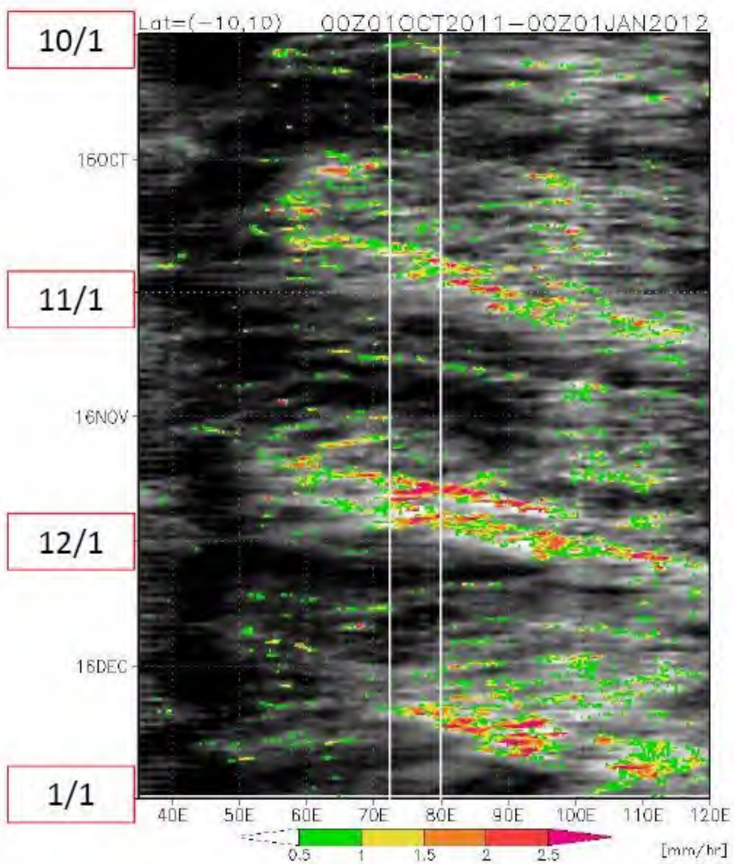

Kunio Yoneyama and Chidong Zhang (2012 DYNAMO)

Hierarchical Tropical Convection

Time-longitude section of transient OLR averaged between the equator and 5N fror May to July in 1980. (Nakazawa, 1988)

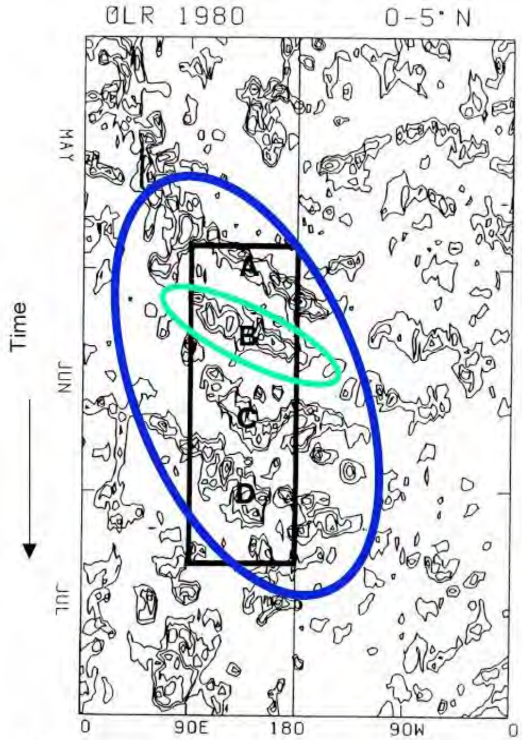

Fig. 1. Time-longitude section of transient (seasonal trend removed) OLR averaged between the equator and 5°N from May to July in 1980. Negative (active convective) regions are contoured. Contour interval decrements of 30 Wm^{-2} starting at $-15\ Wm^{-2}$. Symbols A to D indicate super clusters.

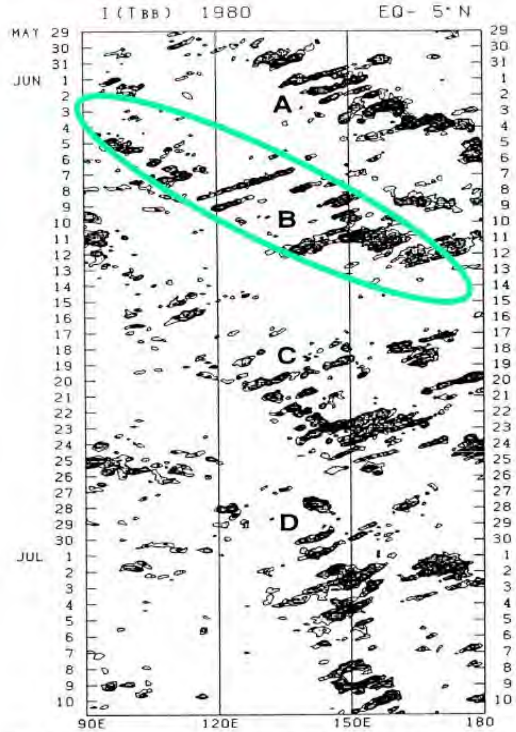

Fig. 2. Time-longitude section of T_{BB} index (I_{TBB}) integrated between the equator and 5°N obtained from the 3-hourly GMS IR data from 29 May 00Z to 10 July 21Z, 1980. Symbols A to D denote the same super cluster as in Fig. 1. Contour interval is 10, and shading denotes the region where values are greater than 20.

Observed multi-scale structure of MJO convective complex

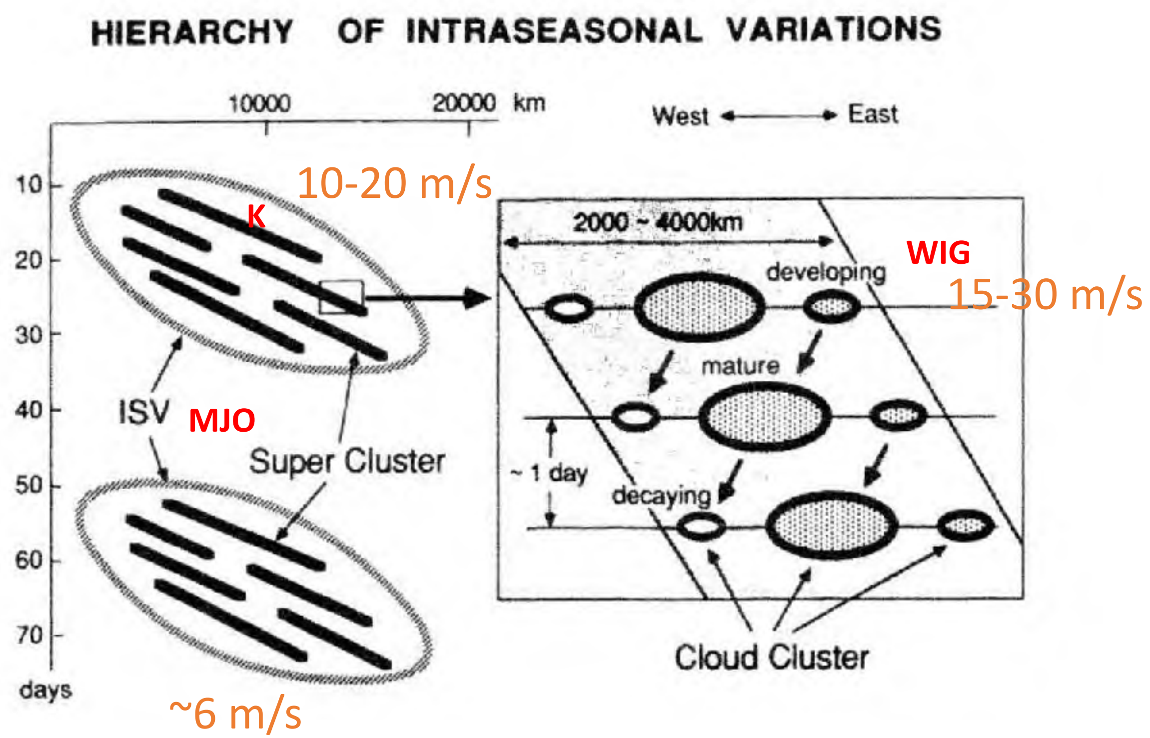

Nakazawa (1988)

Spatio-temporal wavelet transform (STWT)

$$W(b,\tau;a,c)=\int_{-\infty}^{\infty}\int_{-\infty}^{\infty} f(x,t)\psi^{*}_{b,\tau;a,c}(x,t)\,dxdt$$

$$\psi^{*}_{b,\tau;a,c}(x,t)=\frac{1}{a}\psi^{*}\left(\frac{x-b}{ac^{1/2}},\frac{t-\tau}{ac^{-1/2}}\right)$$

Kikuchi, K., and B. Wang 2010
J. Climate, 23, 3814-3834
Spatio-temporal wavelet transform and the multi-scale behavior of the Madden-Julian Oscillation

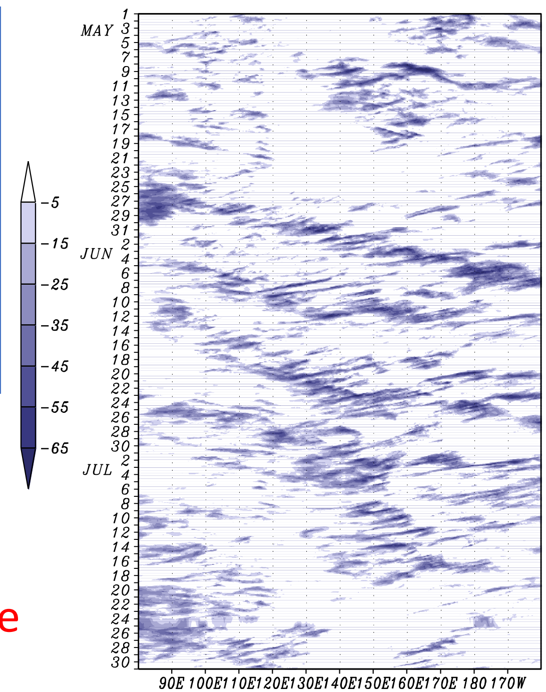

Nakazawa case revisit: GMS IR ¼ degrees, 3 hrs

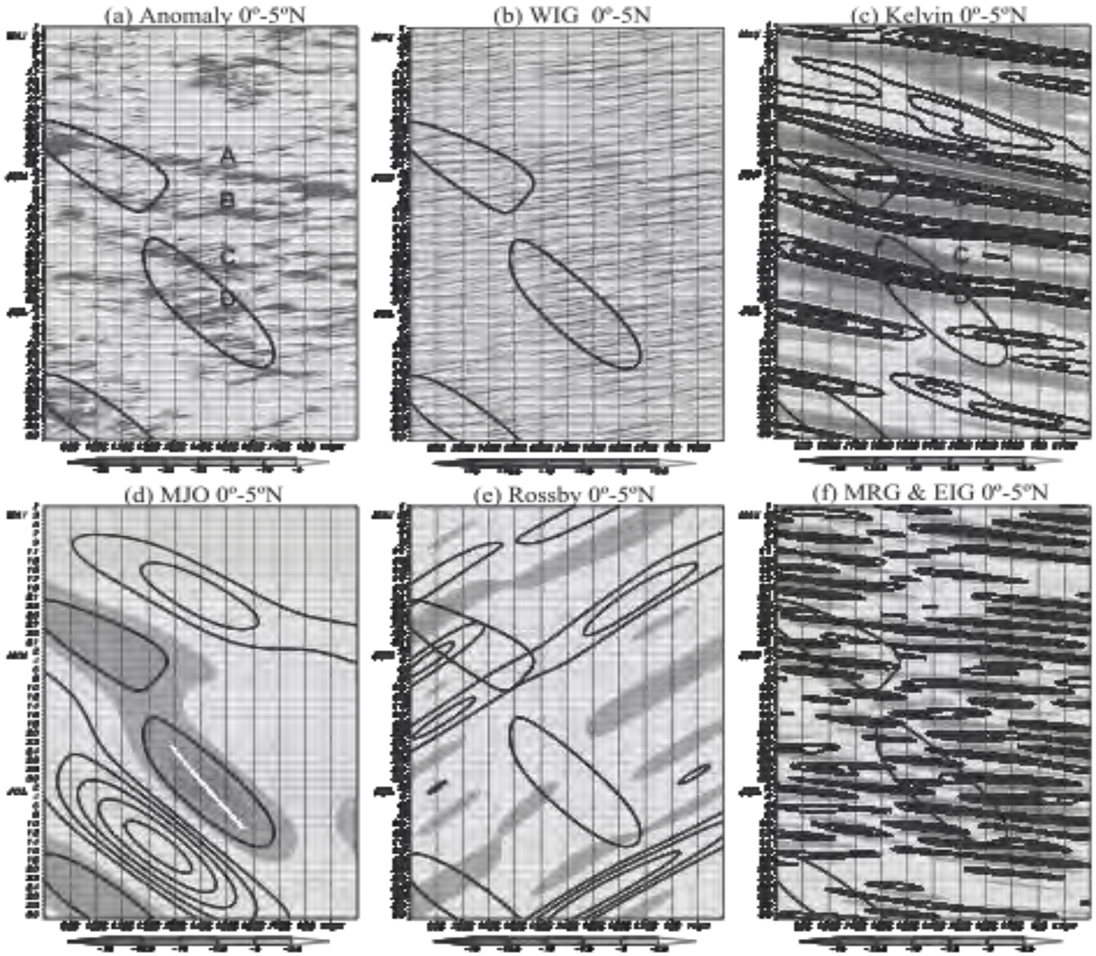

Hovmö ller diagram of GMS IR (K) averaged between 08 and 58N of (a) the original data with the May–July mean removed and (b)–(f) its filtered components: (b) WIG waves, (c) Kelvin waves, (d) the MJO, (e) Rossby waves, and (f) MRG and EIG waves. Labels ''A'' to ''D'' in (a) and (d) are the same as the labels used in Fig. 1 of Nakazawa (1988), indicating the four super cloud clusters. White lines in (c) and (d) are phase lines along with the Kelvin wave and MJO, respectively, drawn with reference to their amplitudes, which will be used in the composite later (e.g., Fig. 7). The contour lines of the MJO at 25 W m22 are superimposed by thick solid curves for reference.

KIKUCHI AND WANG 2010: Spatiotemporal Wavelet Transform and the Multiscale Behavior of the Madden–Julian Oscillation* J. Climate

Atmospheric Equatorial Waves

1. Equations governing tropical atmospheric motion
2. Equatorial kelvin waves
3. General solution
    - 3a. Horizontal structure
    - 3b. Dispersion diagram
4. Low-frequency Equatorial Rossby Waves
5. High-frequency Inertio-Gravity Waves
6. Mixed Rossby-gravity waves (Yanai waves)
7. How mean flow can change the EWs

1. The two-level model for the atmosphere in p-coordinates

- This is the simplest mathematical approximation to a vertically continuous atmospheric motion, which was first advanced by Phillips (1954). The *linear equations in p-coordinates for adiabatic and frictionless motion* are

$$\frac{\partial u}{\partial t} - fv = -\frac{\partial \phi}{\partial x} \qquad (3.5.1a)$$

$$\frac{\partial v}{\partial t} + fu = -\frac{\partial \phi}{\partial y} \qquad (3.5.1b)$$

$$\frac{\partial}{\partial t}\left(\frac{\partial \phi}{\partial p}\right) + \sigma\omega = 0 \qquad (3.5.1c)$$

$$\frac{\partial u}{\partial x} + \frac{\partial v}{\partial y} + \frac{\partial \omega}{\partial p} = 0 \qquad (3.5.1d)$$

where $\sigma = -\frac{\alpha}{\theta}\frac{\partial \theta}{\partial p}$ is the static stability parameter (note, the model includes temperature change). The temperature has been expressed as a function of $\partial\phi/\partial p$ in terms of the equation of state.

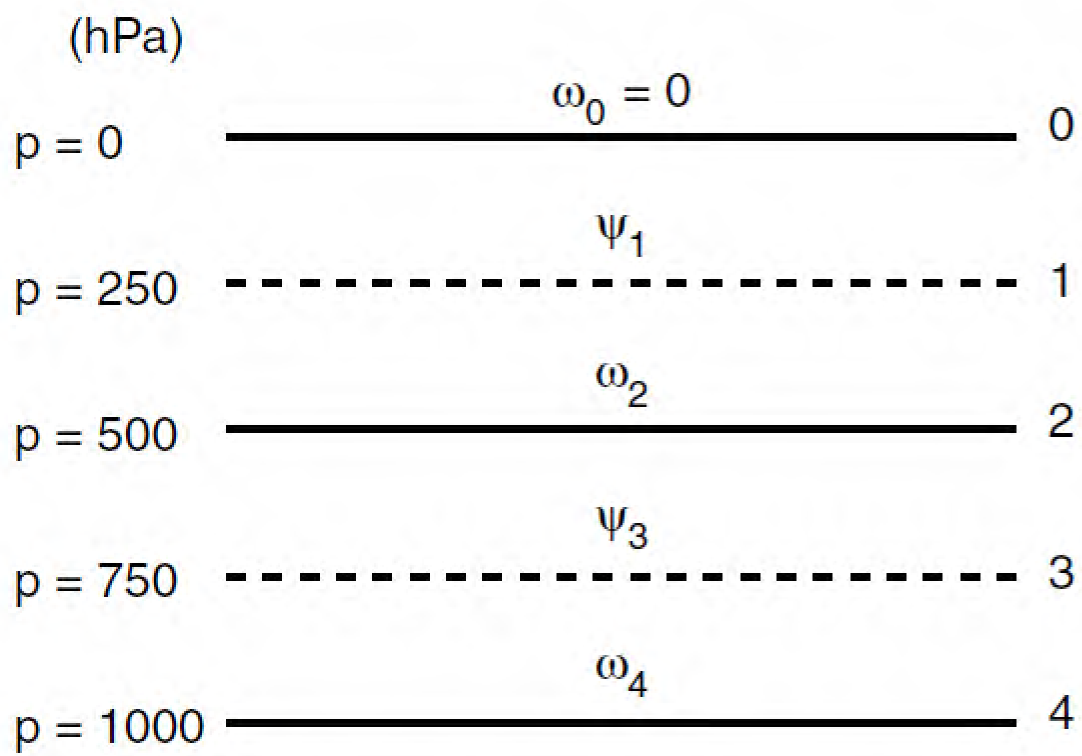

Fig. 8.2 Arrangement of variables in the vertical for the two-level baroclinic model.

- Using a finite difference approximation to the vertical derivatives, write the horizontal momentum equations and continuity equation at level 1 and 3, and thermo-dynamic equation at level 2, using vertical B.C.'s (3.5.2a,b), we have

$$\frac{\partial u_1}{\partial t} - f v_1 + \frac{\partial \phi_1}{\partial x} = 0 \tag{3.5.3a}$$

$$\frac{\partial v_1}{\partial t} + f u_1 + \frac{\partial \phi_1}{\partial y} = 0 \tag{3.5.3b}$$

$$\frac{\partial u_1}{\partial x} + \frac{\partial v_1}{\partial y} + \frac{\omega_2}{\Delta p} = 0 \tag{3.5.3c}$$

$$\frac{\partial u_3}{\partial t} - f v_3 + \frac{\partial \phi_3}{\partial x} = 0 \tag{3.5.3d}$$

$$\frac{\partial v_3}{\partial t} + f u_3 + \frac{\partial \phi_3}{\partial y} = 0 \tag{3.5.3e}$$

$$\frac{\partial u_3}{\partial x} + \frac{\partial v_3}{\partial y} - \frac{\omega_2}{\Delta p} = 0 \tag{3.5.3f}$$

$$\frac{\partial}{\partial t}(\phi_3 - \phi_1) + \sigma_2 \Delta p \omega_2 = 0 \tag{3.5.3g}$$

- Taking the differences, (3.5.3d)-(3.5.3a) and (3.5.3e)-(3.5.3b), and using the continuity relation (3.5.3c) and (3.5.3f) in (3.5.3g), we obtain equations for the baroclinic component:

$$\frac{\partial \tilde{u}}{\partial t} - f\tilde{v} + \frac{\partial \tilde{\phi}}{\partial x} = 0 \tag{3.5.4a}$$

$$\frac{\partial \tilde{v}}{\partial t} + f\tilde{u} + \frac{\partial \tilde{\phi}}{\partial y} = 0 \tag{3.5.4b}$$

$$\frac{\partial \tilde{\phi}}{\partial t} + c_1^{\,2}\left(\frac{\partial \tilde{u}}{\partial x} + \frac{\partial \tilde{v}}{\partial y}\right) = 0 \tag{3.5.4c}$$

where

$$c_1 \equiv \sqrt{\sigma_2 \Delta p^2 / 2} \tag{3.5.5a}$$

and

$$\tilde{u} \equiv u_3 - u_1 \qquad \tilde{v} \equiv v_3 - v_1 \qquad \tilde{\phi} \equiv \phi_3 - \phi_1 \tag{3.5.5b}$$

- $\tilde{u}$ and $\tilde{v}$ are zonal and meridional thermal winds, $\tilde{\phi}$ is thickness, and c_1 represents the **speed of internal gravity waves.** Equations (3.5.4a,b,c) describe the **first (lowest) baroclinic mode.**

The equation is the same form as those of **shallow water equations** except that the parameter c_1 differs from that of the shallow-water model. Taking $\Delta p = 400\,\mathrm{mb}$, $\sigma = 3 \times 10^{-2}\ \mathrm{m^2 s^{-2} mb^{-2}}$, $c_1 \approx 50\,\mathrm{ms^{-1}}$. This is the internal gravity wave speed for a dry atmosphere.Taking the density scale height $H = 9\,\mathrm{km}$, the external gravity wave speed in the shallow-water model is $c_0 \approx 300\,\mathrm{ms^{-1}}$. Thus, $c_1 << c_0$.

- We shall use a shallow-water equatorial beta-plane model to discuss equatorial waves.
- The model equations in a linear framework can be written as

$$\frac{\partial u}{\partial t} - \beta y v = -\frac{\partial \phi}{\partial x} \qquad (4.7.1a)$$

$$\frac{\partial v}{\partial t} + \beta y u = -\frac{\partial \phi}{\partial y} \qquad (4.7.1b)$$

$$\frac{\partial \phi}{\partial t} + C_0^2\left(\frac{\partial u}{\partial x} + \frac{\partial v}{\partial y}\right) = 0 \qquad (4.7.1c)$$

where C_0 is the long gravity wave speed, either for external or internal modes. Depending on different vertical modes, it can take on different values.

- There are two parameters in (4.7.1), β and C_0, which form two intrinsic scales: a length scale $L=\sqrt{C_0/\beta}$ (**equatorial Rossby radius of deformation**) and a time scale $\tau = 1\big/\sqrt{\beta C_0}$, where C_0 is the velocity scale for the wave motion and C_0^2 is a scale for ϕ. Using these scales, write

$$(x, y) = \sqrt{\frac{C_0}{\beta}}(x', y')$$

$$t = t' / \sqrt{\beta C_0} \qquad (4.7.2)$$

$$(u, v) = C_0(u', v')$$

$$\phi = C_0^2 \phi' \quad \text{(ageostrophic scaling)}$$

where the prime denotes non-dimensional quantities.

The non-dimensional equation of (4.7.1a,b,c) become

$$\frac{\partial u'}{\partial t'} - y'v' = -\frac{\partial \phi'}{\partial x'} \tag{4.7.3a}$$

$$\frac{\partial v'}{\partial t'} + y'u' = -\frac{\partial \phi'}{\partial y'} \tag{4.7.3b}$$

$$\frac{\partial \phi'}{\partial t'} + \frac{\partial u'}{\partial x'} + \frac{\partial v'}{\partial y'} = 0 \tag{4.7.3c}$$

The domain is a horizontally infinite equatorial beta-plane. Matsuno (1966) proposed the adequate side boundary conditions:

$$u', v', \phi' \text{ are bounded as } y \to \pm\infty. \tag{4.7.4}$$

- In the real atmosphere, the position of the poles puts an upper limit on $|y|$ so rigorous boundary conditions should be different. However, the approximate condition (4.7.4) has little effect on the solutions of the lower y-modes, as will be seen later.

2. Equatorial Kelvin waves

In the previous section, we have learned that the existence of a side boundary is responsible for coastal Kelvin waves, which only have along-boundary motion (no motion in the direction perpendicular to the side boundary).

- In this subsection we first examine a special case in which the meridional motion is identically zero, $v' \equiv 0$, i.e., the motion is exactly in the along-equator direction. Then the system of equation (4.7.3a,b,c) becomes

$$\frac{\partial u'}{\partial t'} = -\frac{\partial \phi'}{\partial x'} \qquad (4.7.5a)$$

$$y'u' = -\frac{\partial \phi'}{\partial y'} \qquad (4.7.5b)$$

$$\frac{\partial \phi'}{\partial t'} + \frac{\partial u'}{\partial x'} = 0 \qquad (4.7.5c)$$

Equation (4.7.5) implies that the motion is in geostrophic balance even near the equator.

- The combination of (4.7.5a) and (4.7.5c) yields the wave equation

$$\frac{\partial^2 u'}{\partial t'^2} - \frac{\partial^2 u'}{\partial x'^2} = 0$$

- The general solution of this system is

$$u' = F(x' \mp t')Y(y')$$

where F is an arbitrary function. Substituting this into (4.7.5a), we find

$$\phi' = \pm u'$$

- From (4.7.5b), one then finds that

$$y'Y(y') \pm \frac{dY}{dy'} = 0$$

from which

$$Y(y') = Y(0)e^{\mp y'^2/2}$$

- We choose only the "-" sign because the other choice leads to an unbounded solution for large y . The solution of the system is of the form

$$u' = \phi' = F(x' - t')e^{-y'^2/2} \qquad (4.7.6)$$

or in dimensional form

$$u = \phi / C_0 = F(x - C_0 t)e^{-\beta y^2 / 2C_0}, \quad v \equiv 0 \qquad (4.7.7)$$

- The waves represented by (4.7.7) are called **Equatorial Kelvin waves,** because the governing equations (4.7.5a,b,c) are identical to those of coastal Kelvin waves except the Coriolis force in this case is βy. The following properties of the equatorial Kelvin wave are also similar to **coastal Kelvin waves** if we regard the equator as a rigid side-wall boundary.

- Some remarks are made as follows.

(A) The equatorial Kelvin waves move eastward with the phase speed of gravity waves, C_0.

(B) The Kelvin waves are trapped near the equator with an e-folding scale of $\sqrt{2C_0/\beta}$. For the atmosphere, $C_0 \approx 50\, ms^{-1}$, $\sqrt{2C_0/\beta} \approx 2000\, km$, while for the ocean $C_0 \approx 2.5\, ms^{-1}$, $\sqrt{2C_0/\beta} \approx 46\, km$. Higher-order baroclinic modes are even more tightly trapped near the equator.

(C) $v = 0$, while u is exactly in geostrophic balance with ϕ. Facing the moving direction, high pressure is to the right (left) in the northern (southern) hemisphere.

(D) Kelvin waves are **non-dispersive** because F represents an arbitrary wave-packet that propagates without changing shape. This means that the group speed equals the phase speed, i.e., the energy is also propagated with a speed C_0.

(E) Physically, the equatorial Kelvin waves are just a long gravity wave trapped to the equator because of Earth's rotation via geostrophic balance described in (4.7.5b). It reveals an important property of the equatorial zone: it acts as a wave guide. [This idea seems to have been first put forward by Yoshida in 1959].

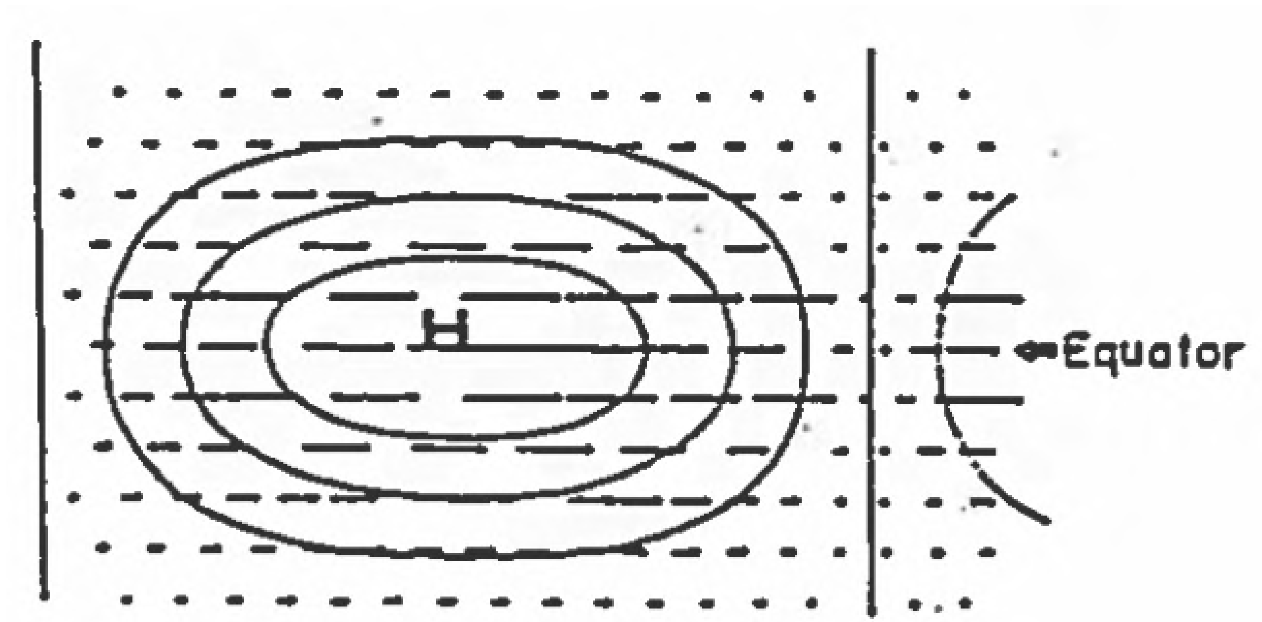

Fig. 1 Pressure and velocity fields of Equatorial Kelvin waves (matsuno, 1996)

Fig.1 shows the horizontal structure of velocity and pressure characteristic of Kelvin waves (Matsuno, 1966).

(1) The zonal velocity and pressure distributions are symmetric about the equator but the meridional velocity v is identically zero.

(2) High (low) pressure is accompanied by west (east) wind.

(3) At both ends of the pressure system, the features of a <u>pure gravity wave are marked</u>, while in the central part of the cell where the longitudinal pressure gradient is weak and zonal velocity is strong, the geostrophic balance is pronounced. The latter becomes more dominant for long Kelvin waves.

3. General solution: dispersion relation

We now examine the general case in which v does not vanish. Since the coefficients of (4.7.3a,b,c) are y-dependent only, separation of y-dependent and x-dependent parts to the wave solution is possible.

- Therefore, we search for a wave solution of the form

$$(u', v', \phi') = \mathrm{Re}(U(y), V(y), \Phi(y))e^{i(kx-\omega t)} \tag{4.7.8}$$

From (4.7.4),

$U(y), V(y), \Phi(y)$ are bounded, as $y \to \pm\infty$. (4.7.9)

Substituting (4.7.8) into (4.7.3) yields

$$-i\omega U - yV = -ik\Phi \tag{4.7.10a}$$

$$-i\omega V + yU = -d\Phi / dy \tag{4.7.10b}$$

$$-i\omega\Phi + ikU + dV / dy = 0 \tag{4.7.10c}$$

- It is most convenient to eliminate U and Φ in order to formulate a single equation for V. Solving for U and Φ from (4.7.10a) and (4.7.10c) leads to

$$U = \frac{1}{k^2 - \omega^2}\left(ik\frac{dV}{dy} - i\omega yV \right) \qquad (4.7.11a)$$

$$\Phi = \frac{1}{k^2 - \omega^2}\left(i\omega\frac{dV}{dy} - ikyV \right) \qquad (4.7.11b)$$

Using (4.7.11a,b) in (4.7.10b), we find

$$\frac{d^2V}{dy^2} + \left[(\omega^2 - k^2) - \frac{k}{\omega} - y^2 \right] V = 0 \qquad (4.7.12)$$

Note that in deriving Equation (4.7.11), $k^2 \neq \omega^2$ is assumed.

- Equation (4.7.12) along with the boundary condition for V, (4.7.9), poses an eigenvalue problem, which is the same as the Schrödinger equation for a simple harmonic oscillator. The boundary conditions (4.7.9) are satisfied only when

$$\omega^2 - k^2 + k/\omega = 2m+1, \qquad m = 0,1,2,\ldots \qquad (4.7.13)$$

which determines the eigenvalue ω for a given k. Let

$$V(y) = V_m(y) = e^{-y^2/2} H_m(y), \qquad m = 0,1,2,\ldots \qquad (4.7.14)$$

- From (4.7.12), $H_m(y)$ satisfies the Hermite Equation,

$$\frac{d^2H}{dy^2} - 2y\frac{dH}{dy} + 2mH = 0 \qquad (4.7.15)$$

The corresponding eigen-solution of (4.7.15) is given by (Abramowitz and Stegan, p.781) the mth Hermite polynomial:

$$H_m(y) \equiv \sum_{l=0}^{[m/2]} \frac{(-1)^l m!}{l!(m-2l)!}(2y)^{m-2l} \qquad (4.7.16)$$

The first 6 order's are

$$H_0(y) = 1$$

$$H_1(y) = 2y$$

$$H_2(y) = 4y^2 - 2$$

$$H_3(y) = 8y^3 - 12y$$

$$H_4(y) = 16y^4 - 48y^2 + 12$$

$$H_5(y) = 32y^5 - 160y^3 + 20y$$

Since

$$\int_{-\infty}^{\infty} H_m(y) H_n(y) e^{-y^2} dy = \begin{cases} 0, & m \neq n \\ 2^m m! \sqrt{\pi}, & m = n \end{cases} \qquad (4.7.17)$$

thus let $V_m(y) \equiv e^{-y^2/2} H_m(y) / \sqrt{2^m m! \sqrt{\pi}}$,

then

$$\int_{-\infty}^{\infty} V_m(y) V_n(y) dy = \begin{cases} 0, & m \neq n \\ 1, & m = n \end{cases} \qquad (4.7.18)$$

3a. Horizontal structure

The meridional velocity $V(y)$ for the mth eigen-solution, $V_m(y)$ is described by equations (4.7.14) and (4.7.16). Notice that $V_m(y)$ with m even (odd) is an even (odd) function of y in $(-\infty, \infty)$ with m **nodal points.** The values $y = \sqrt{2m+1}$ are turning latitudes: $V_m(y)$ is oscillatory in the interval $|y| < \sqrt{2m+1}$ and exhibits evanescent (monotonic) decay for $|y| > \sqrt{2m+1}$. Obviously, the lower modes are equatorially trapped, since for large y the waves decay exponentially in amplitude.

- $U(y)$ and $\Phi(y)$ can be obtained from equations (4.7.11a,b). In establishing U_m and $\Phi_m(y)$, it is convenient to use the following recurrence relation for Hermite's polynomial

$$\frac{dH_m(y)}{dy} = 2mH_{m-1}(y) \qquad (4.7.19a)$$

$$H_{m+1}(y) = 2yH_m(y) - 2mH_{m-1}(y) \qquad (4.7.19b)$$

For $m \geq 1$, the u' , ϕ' and v' fields are (from Eq. (4.7.8))

$$v'_m = \mathrm{Re}\, V_m(y) e^{i(kx-\omega t)} \qquad (4.7.20a)$$

$$u'_m = \mathrm{Re}\frac{i}{2}\left[\frac{V_{m+1}}{\omega - k} + \frac{2m}{\omega + k}V_{m-1}\right]e^{i(kx-\omega t)} \qquad (4.7.20b)$$

$$\phi'_m = \mathrm{Re}\frac{i}{2}\left[\frac{V_{m+1}}{\omega - k} - \frac{2m}{\omega + k}V_{m-1}\right]e^{i(kx-\omega t)} \qquad (4.7.20c)$$

3b. Dispersion diagram

Equation (4.7.13) is the dispersion equation (non-dimensional), which describes the relationship between wavenumber and frequency. For convenience, we specify ω to be always positive while k can be either positive (corresponding eastward propagation) or negative (corresponding westward propagation). The frequency ω as a function of k is plotted in Fig.2.

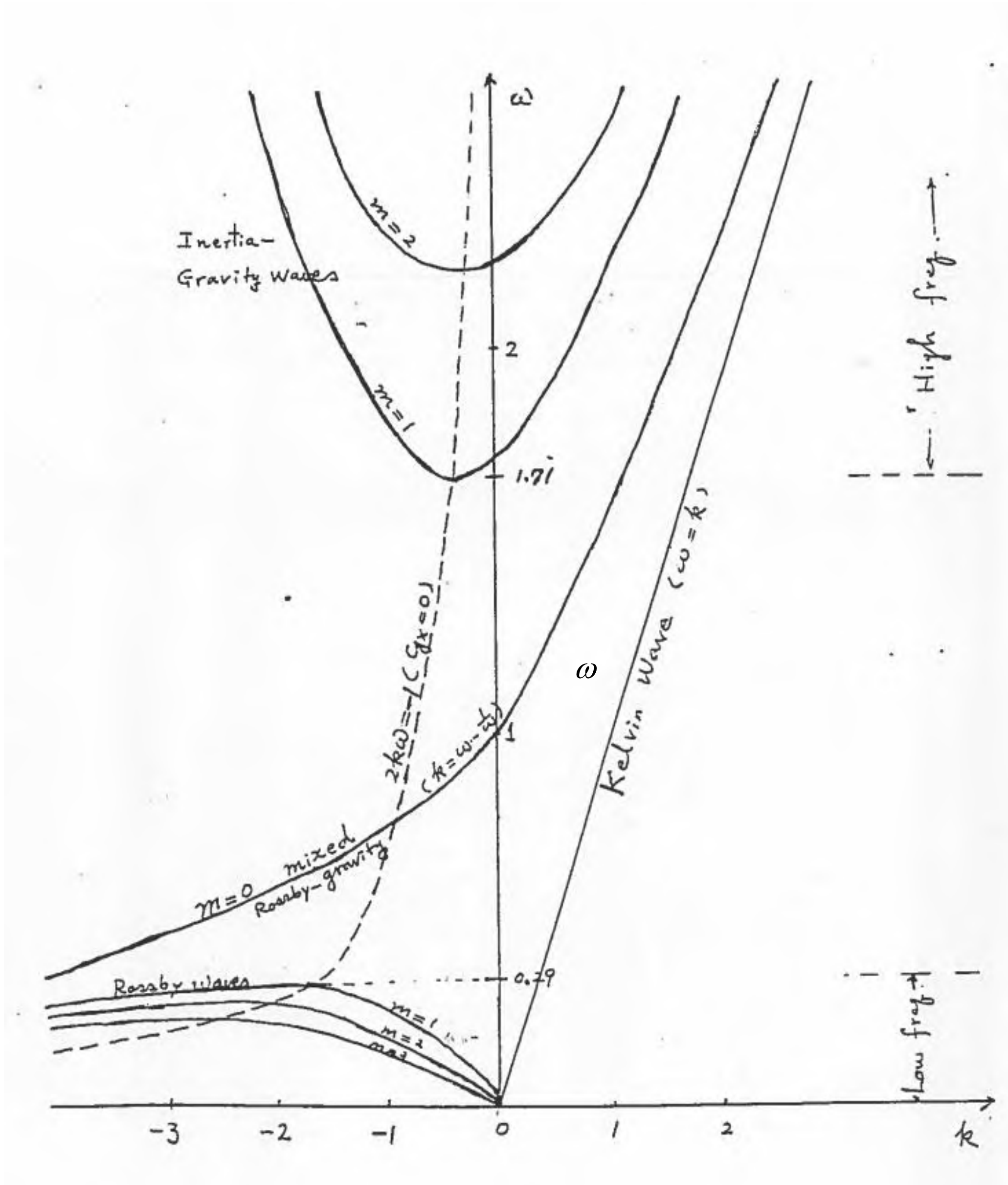

Fig. 2 Dispersion diagram for equatorial waves. Assuming k is real, and ω >0

- The dispersion equation (4.7.13) suggests three different types of equatorial waves.
- We first examine the $m \geq 1$ cases (modes). When $m \geq 1$, the exact dispersion relation is given by

$$k_m = -\frac{1}{2\omega} \pm \sqrt{\omega^2 + 1/4\omega^2 - (2m+1)} \qquad m = 1,2,3,\ldots \qquad (4.7.21)$$

To obtain a real (number) k, which corresponds to propagating neutral waves (non-decaying), one must require that

$$\omega^2 + \frac{1}{4\omega^2} - (2m+1) \geq 0$$

i.e.

$$\omega \geq \sqrt{\frac{m+1}{2}} + \sqrt{\frac{m}{2}} \geq 1 + \frac{1}{\sqrt{2}}, \quad m = 1,2,\ldots \qquad (4.7.22a)$$

or

$$\omega \leq \sqrt{\frac{m+1}{2}} - \sqrt{\frac{m}{2}} \leq 1 - \frac{1}{\sqrt{2}}, \quad m = 1,2,\ldots \qquad (4.7.22b)$$

Equations (4.7.20a,b) imply that there are two distinguished groups of waves: one is high frequency, $\omega \geq 1 + 1/\sqrt{2}$, and the other is low frequency, $\omega \geq 1 + 1/\sqrt{2}$.

- If the dispersion equation, (4.7.13), is differentiated with respect to k , one finds that the group speed in the x-direction is

$$C_{gx} \equiv \frac{\partial w}{\partial k} = \frac{2k\omega + 1}{2\omega^2 + k/\omega} \qquad (4.7.23)$$

which vanishes at

$$2k\omega = -1 \text{ (if } 2\omega^2 + k/\omega \neq 0 \text{)} \qquad (4.7.24)$$

The curve $\omega = -1/2k$ is shown in Fig.3 by the dashed line. Note also that $\partial\omega/\partial k = 0$ is a necessary condition for ω to obtain extrema! One can find out the values of extrema simply by putting $k = -1/2\omega$ into (4.7.19).

- Extrema for ω are

$$\omega_{extrema} = \begin{cases} \sqrt{\frac{m+1}{2}} + \sqrt{\frac{m}{2}}, & \text{for high frequency mode} \\ \sqrt{\frac{m+1}{2}} - \sqrt{\frac{m}{2}}, & \text{for low frequency mode} \end{cases} \qquad (4.7.25)$$

It can be further shown that the points

$$\left(k = -\frac{1}{2\omega},\ \sqrt{\frac{m+1}{2}} + \sqrt{\frac{m}{2}}\ \right) \qquad (4.7.26a)$$

correspond to minima for high frequency waves, while the points

$$\left(k = -\frac{1}{2\omega},\ \sqrt{\frac{m+1}{2}} - \sqrt{\frac{m}{2}}\right) \qquad (4.7.26b)$$

correspond to maxima for low frequency waves.

4. Low-frequency Equatorial Rossby Waves

These correspond to the lower branches in the dispersion diagram. The non-dimensional frequency of these waves is smaller than $1-1/\sqrt{2}=0.29$, thus the dimensional frequency $\omega_* \le 0.29\sqrt{\beta C_0}$. Taking $C_0 = 50\,\mathrm{ms}^{-1}$ for the atmosphere, $\omega_* \le 10^{-5}s^{-1}$ or the period $T_* \ge 7.3\,\mathrm{days}$; taking $C_0 = 2.5\,\mathrm{ms}^{-1}$ for the ocean, $\omega_* \le 2.15\times 10^{-5}s^{-1}$ or the period $T_* \ge 34\,\mathrm{days}$.

- For low frequency waves, ω is small, thus $\omega^2 << 1/\omega^2$. The dispersion equation can then be approximated by

$$k_{m\pm} = -\frac{1}{2\omega} \pm \sqrt{\frac{1}{4\omega^2} - (2m+1)} < 0 \qquad (4.8.1a)$$

or

$$\omega = -\frac{k_m}{k_m{}^2 + (2m+1)} \qquad (4.8.1b)$$

- The higher the index of the vertical mode m, the lower the frequency ω. The fractional error of (4.8.1a,b) has a maximum value for $m=1$ of less than 3%.

- Resuming the dimensional form, the phase speed is

$$\frac{\omega_*}{k_*} = -\frac{\beta}{k_*^2 + \frac{\beta}{C_0}(2m+1)} \qquad (4.8.2)$$

which is the same as a Rossby wave in a beta-plane channel except the quantized y-wavenumber has a slightly different form due to the side boundary condition at $y = \pm\infty$. These low-frequency modes are, therefore, called **equatorial Rossby waves.** They occur because f varies with latitude.

- Equation (4.8.2) indicates that these waves are always westward propagating. As shown in the previous section, §4.7, the frequency ω for Rossby waves reaches maxima (the frequency at which the group speed is zero) at

$$\omega = \sqrt{\frac{m+1}{2}} - \sqrt{\frac{m}{2}}$$

- Thus, for **long Rossby waves** with k_{m+} (taking "+" sign in (4.8.1a)), the group velocity is westward (the slope is negative on the dispersion curve in Fig.1) while for **short Rossby waves** with k_{m-} (taking "-" sign in (4.8.1a)) the group velocity is eastward (the slope is positive).

- For long Rossby waves, $k \to 0$, so that

$$\frac{\omega}{k} \approx -\frac{1}{2m+1} \quad (\; m = 1, 2, ...) \qquad (4.8.3)$$

implying that they are approximately non-dispersive. The dimensional westward phase speed is $(2m+1)^{-1}$ times the long gravity wave speed C_0. Thus, the wave speed is at most one-third of the long gravity wave speed. For example, if $C_0 = 2.5\,\mathrm{ms}^{-1}$ for the first baroclinic mode in the equatorial Pacific Ocean, the $m = 1$ Rossby wave speed is approximately $0.8\mathrm{ms}^{-1}$; corresponding to a time of 6 months to cross the Pacific basin from east to west.

- Fig.3 depicts geopotential and velocity distributions for $m=1$ (left panel) and $m=2$ (right panel) modes for equatorial Rossby waves (after Matsuno, 1966). The figure was drawn using Eqns.(4.7.26a,b,c) in the previous section.

- The Rossby waves are characterized by a geostrophic relationship between pressure and wind fields. Strong zonal winds are found near equator for the $m=1$ mode, which is expected from approximate balance between pressure gradient and Coriolis forces (both of them approach zero as $y \to 0$). For the $m=1$ mode, u and ϕ are symmetric, v is antisymmetric, while for the $m=2$ mode, u and ϕ are antisymmetric about the equator but v is symmetric. There is no meridional motion at the equator for the $m=1$ mode. What about the $m=2$ mode?

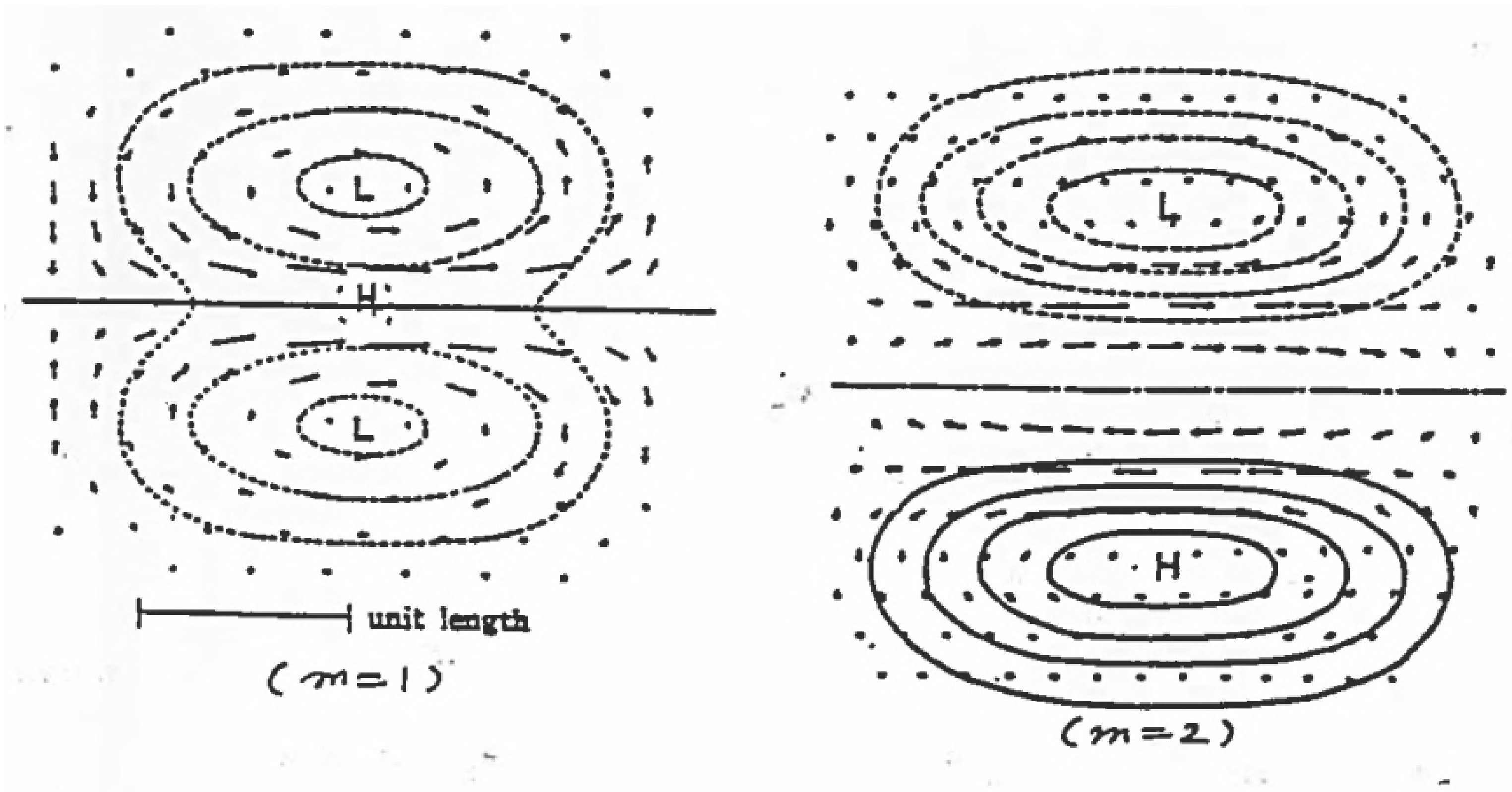

Fig. 3 Equatorial Rossby waves (m=1 and m=2) (Matsuno,1996)

5. High-frequency Inertio-Gravity Waves

- These are the upper branches in Fig.1, whose frequencies exceed $1+1/\sqrt{2}=1.71$, or dimensionally, $\omega_* > 1.71\sqrt{\beta C_0}$. Taking $C_0 = 50\,\mathrm{ms}^{-1}$ for the atmosphere, $\omega_* \geq 5.77\times 10^{-5} s^{-1}$, or the period $T_* \leq 1.26\,\mathrm{days}$ while for the ocean, $C_0 = 2.5\,\mathrm{ms}^{-1}$, $\omega_* \geq 1.29\times 10^{-5} s^{-1}$ or $T_* \leq 5.63\,\mathrm{days}$. The higher the meridional index m is, the shorter the period.

- For high-frequency waves, where $1/2\omega << 1$, the dispersion relation may be approximated by

$$k_m = \pm\sqrt{\omega^2 - (2m+1)} \qquad (4.8.4a)$$

$$\omega^2 = k_m^2 + (2m+1) \qquad (4.8.4b)$$

The fractional error in making this approximation is bounded by a maximum value of 14% when $m=1$.

In dimensional form, (4.8.4b) gives

$$\frac{\omega_*}{k_*} = \sqrt{C_0^2 + \frac{\beta C_0(2m+1)}{k_{*m}^2}} \qquad (4.8.5)$$

which is similar to the inertio-gravity wave speed in an

$f-$plane,

$$\frac{\omega_*}{k_*} = \sqrt{C_0^2 + \frac{f^2}{k_*^2 + l_*^2}}$$

where C_0 is the pure gravity wave speed (if we identify $\beta C_0(2m+1)$ as f^2 and neglect l^2). Therefore, these high frequency modes are called **inertio-gravity waves**, following Matsuno (1966).

- We note that ω reaches minima at

$$\omega = \sqrt{\frac{m+1}{2}} + \sqrt{\frac{m}{2}}$$

- For gravity waves with

$$k_{m+} = -\frac{1}{2\omega} + \sqrt{\omega^2 + \frac{1}{4\omega^2} - (2m+1)}$$

the group speed C_{gx} is eastward (positive slope on dispersion curve in Fig.1, right branches), whereas for gravity waves with

$$k_{m-} = -\frac{1}{2\omega} - \sqrt{\omega^2 + \frac{1}{4\omega^2} - (2m+1)}$$

(negative slope, left branches) the group speed is <u>westward</u>. These features are important in oceanography when considering wave reflection from meridional coastline. Further discussion of these modes in the ocean can be referred to Gill (1982).

- Fig.4 shows the eastward and westward propagating inertio-gravity waves for $m=1$ and $m=2$ modes. They are essentially **ageostrophic** and exhibit the nature of inertio-gravity waves. The $m=1$ mode is trapped more tightly to the equator. The $m=1$ mode has symmetric structures in u and ϕ but antisymmetric structure in v with respect to the equator. On the other hand, $m=2$ modes have u , ϕ antisymmetric while v is symmetric about the equator.

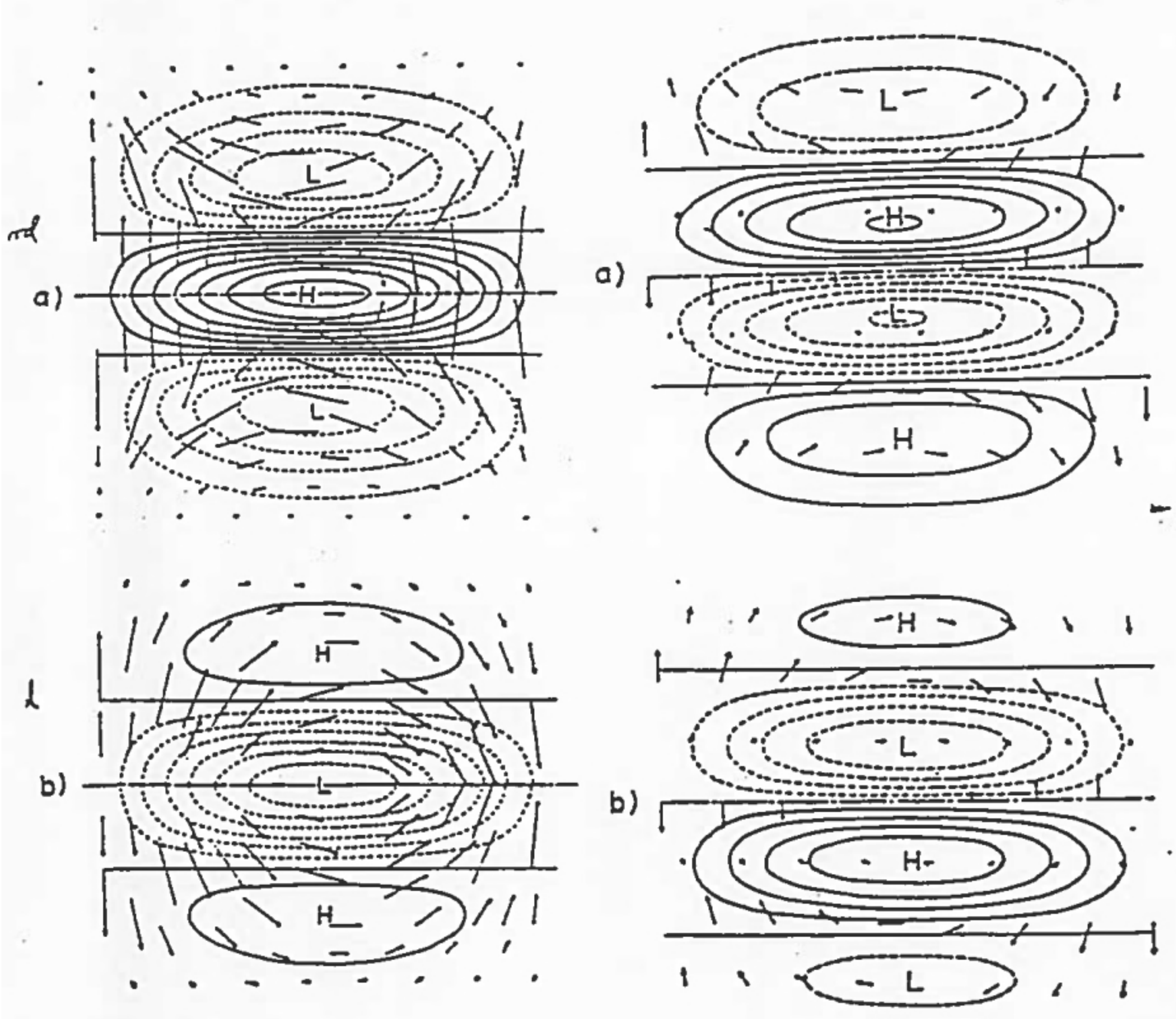

Fig.4 Pressure and velocity distribution of inertial-gravity waves for m=1 (left panel) and m=2 (right panel).

A; Eastward propagating; b:Westward propagating (Matsuno, 19960

- There is a gap in ω between $1-1/\sqrt{2}$ and $1+1/\sqrt{2}$, so that two groups of waves are well separated. In the intermediate frequency band, $1-1/\sqrt{2}<\omega<1+1/\sqrt{2}$,

$$\omega^2+\frac{1}{4\omega^2}-(2m+1)<0 \qquad m=1,2,\ldots$$

Hence

$$k_{m\pm}=-\frac{1}{2\omega}\pm i\sqrt{(2m+1)-\left(\omega^2+\frac{1}{4\omega^2}\right)} \quad (4.8.6)$$

implying a wave propagating westward ($\mathrm{Re}\,k_m=-1/2\omega$) and with amplitude exponentially decaying toward the east or west, depending on the choice of sign.

(Fig.4 Pressure and velocity distributions of inertial-gravity waves for $m=1$ (left panel) and $m=2$ (right panel).

a: eastward propagating; b: westward propagating)

6. Mixed Rossby-Gravity Waves

- We now examine the $m=0$ mode. This is a special mode which has a distinguished nature from the $m \geq 1$ modes in many aspects!

When $m=0$, the dispersion equation $\omega^2 - k^2 - k/\omega = 1$ yields two roots for   :

$$k = \omega - \frac{1}{\omega} \quad \text{and} \quad k = -\omega \qquad (4.8.7)$$

- Recall that in solving the problem we assume that $\omega^2 \neq k^2$, hence, the second root should be rejected.

For the $m=0$ mode, we have

$$V_0(y) = e^{-y^2/2}, \qquad \frac{dV_0}{dy} = \frac{1}{2}V_1 \qquad yV_0 = \frac{1}{2}V_1 \tag{4.8.8a}$$

thus equations (4.7.11a,b) from the previous section gives

$$U = \Phi = \frac{i\omega V_1}{2} \tag{4.8.8b}$$

Therefore,

$$v_0' = \mathrm{Re}\, e^{-y^2/2} e^{i(kx-\omega t)} \tag{4.8.9a}$$

$$u_0' = \phi_0' = \mathrm{Re}\, i\omega V_1(y) e^{i(kx-\omega t)} \tag{4.8.9b}$$

and the solution with is

$$\begin{aligned} v_0' &= \mathrm{Re}\, e^{-y^2/2} e^{i[(\omega-1/\omega)x-\omega t]} \\ u_0' &= \phi_0' = \mathrm{Re}\, i\omega e^{-y^2/2} y e^{i[(\omega-1/\omega)x-\omega t]} \end{aligned} \tag{4.8.10}$$

The dispersion relation (4.8.7) is described by the curve $m=0$ in Fig.1.

- It is interesting to notice that for large ω, one has $k=\omega$, which is the asymptotic limit of high wave-number gravity waves. On the other hand, for small ω, one has $k=-1/\omega$, which is the high wavenumber limit of the Rossby waves. For this reason, this particular $m=0$ mode is called **Mixed Rossby-Gravity waves** or **Yanai waves.** This mixed mode is unique in the equatorial region.
- The crossover point, $\omega=1$, corresponds to a dimensional period $T_*=2\pi/\sqrt{\beta C_0}$, which is about 9.6 days for $C_0=2.5\,\mathrm{ms}^{-1}$ in the ocean and about 2.1 days for $C_0=50\,\mathrm{ms}^{-1}$ in the atmosphere. This is a stationary wave; waves with shorter periods ($k>0$) propagate eastward while waves with periods longer period ($k<0$) propagate westward.

- The group velocity for Yanai waves, however, is always eastward, because

$$\frac{\partial \omega}{\partial k} = \frac{\omega^2}{\omega^2 + 1} > 0 \quad \text{for all } \omega$$

- Fig.5 shows the horizontal distribution of velocity and pressure characteristics of an eastward moving mixed Rossby- Gravity waves (Matsuno, 1966). The pressure and zonal velocity are antisymmetric about the equator while the meridional component v is symmetric. The largest meridional flow occurs near the equator (cross-equatorial flow).
- Fig.5 Pressure and velocity distributions of Mixed Rossby-Gravity waves:

  (a) eastward moving ($k = 0.5$);

  (b) westward moving ($k = -0.5$).

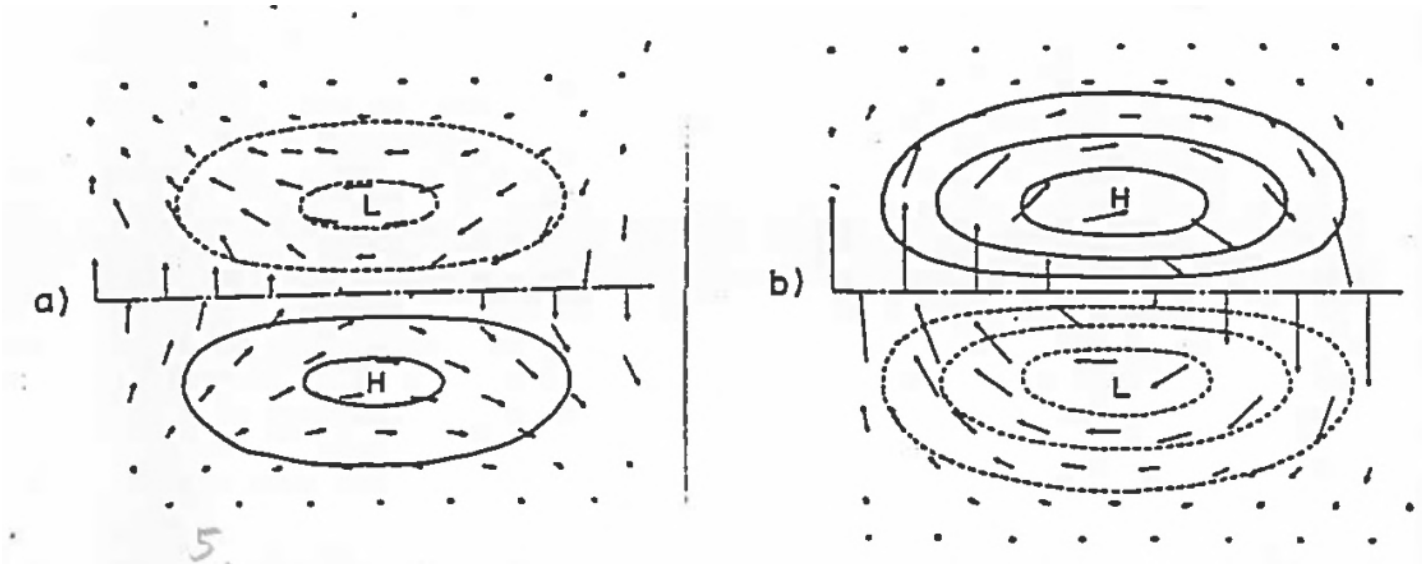

Fig. 5 Pressure and velocity distribution of mixed Rossby-gravity waves: (a) eastward moving (k=0.5); (b)westward moving (k=-0.5)

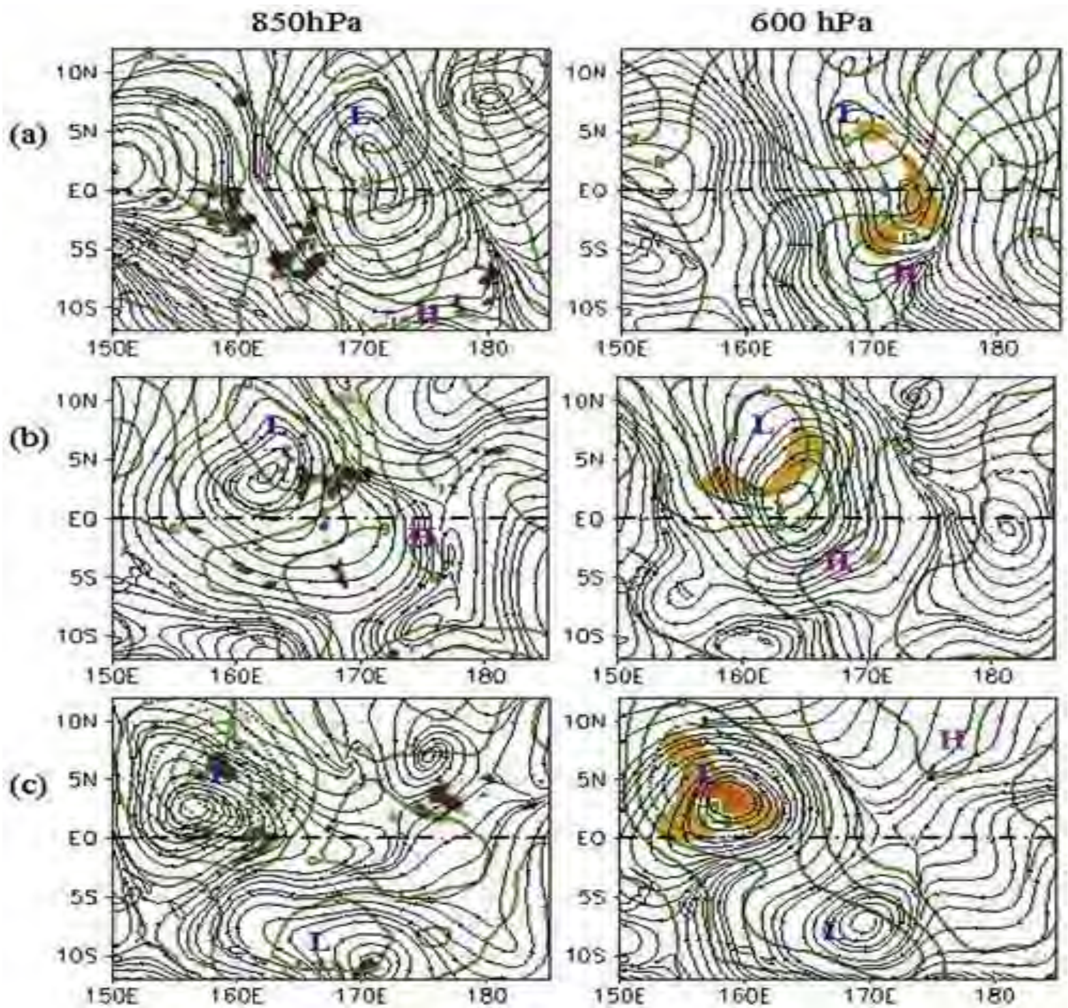

Wind anomaly (streamline), geopotential height anomaly (contour) at (left) 850 hPa and (right) 600 hPa on (a) 12Z 25 Nov., (b) 12Z 26 Nov., and (c) 12Z 27 Nov. The shadings in Figure 4 (left) are rain rate (>0.3 mm/hr) and in Figure 4 (right) vorticity (>2 ? 10? 5 s? 1).

Zhou and Wang 2007

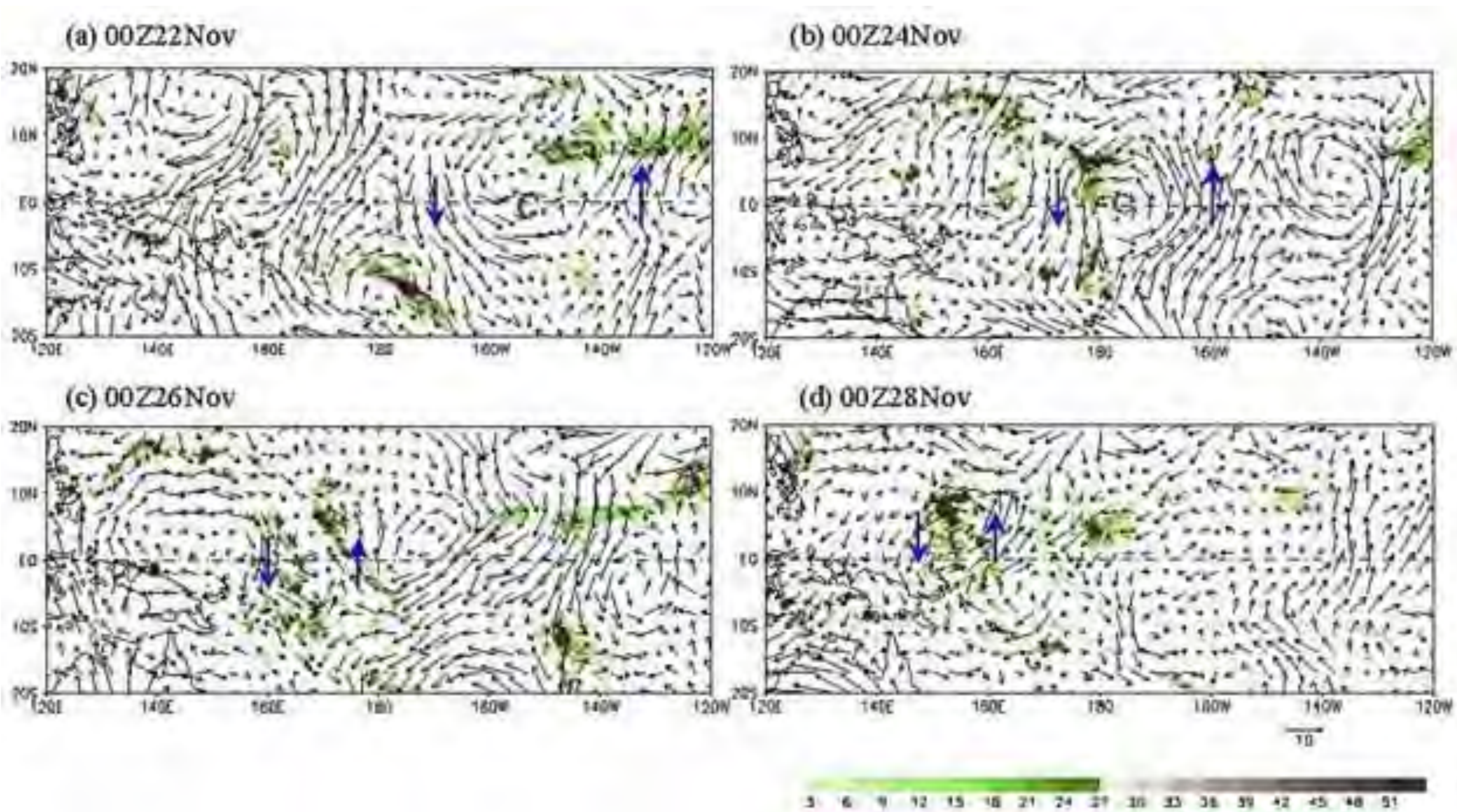

Figure 2. Wind anomaly (streamline) on 500 hPa level and the unfiltered TRMM precipitation rate (shading >0.3 mm/hr) on (a) 00Z 22 Nov. 2004, (b) 00Z 24 Nov. 2004, (c) 00Z 26 Nov. 2004, and (d) 00Z 28 Nov. 2004.

Zhou and Wang 2007

Theoretical Equatorial Waves

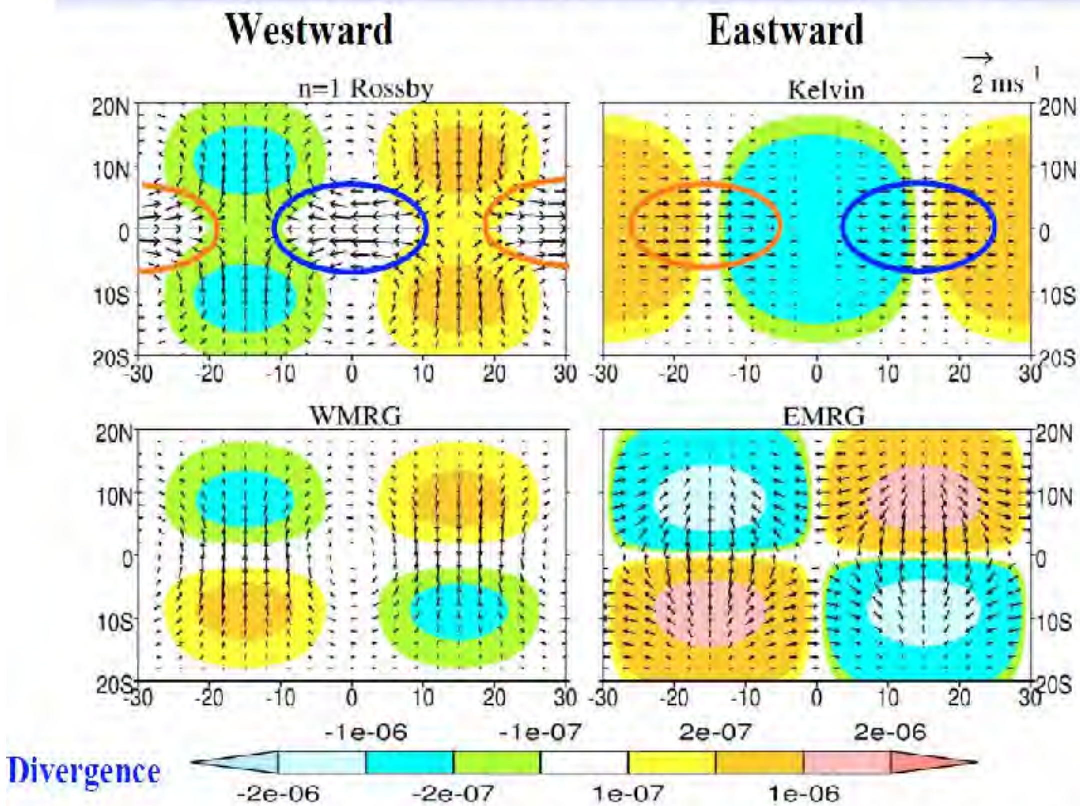

Assumptions: equatorial β-plane, U=0, linear, uniform damping, no forcing

Model for study of effects of Vertical sheared flow

Model formulation including vertical sheared flow

$$\frac{\partial u}{\partial t} + \bar{u}\frac{\partial u}{\partial x} + \omega\frac{\partial \bar{u}}{\partial p} - \beta y v = -\frac{\partial \phi}{\partial x} \qquad \text{(A.3.1a)}$$

$$\frac{\partial v}{\partial t} + \bar{u}\frac{\partial v}{\partial x} + \beta y u = -\frac{\partial \phi}{\partial y} \qquad \text{(A.3.1b)}$$

$$\frac{\partial u}{\partial x} + \frac{\partial v}{\partial y} + \frac{\partial \omega}{\partial p} = 0 \qquad \text{(A.3.1c)}$$

$$\frac{\partial}{\partial t}\left(\frac{\partial \Phi}{\partial p}\right) + \bar{u}\frac{\partial}{\partial x}\left(\frac{\partial \phi}{\partial p}\right) - \beta y v\frac{\partial \bar{u}}{\partial p} + S\omega = 0 \qquad \text{(A.3.1d)}$$

Introduce

$$A_+ = (A_1 + A_3)/2, \qquad A_- = (A_1 - A_3)/2 \qquad \text{(A.3.2)}$$

The two-level model represents two vertical modes, a barotropic mode and a baroclinic mode (A.3.2), which are governed by

Vertical mode interaction under mean vertical shear

The barotropic mode is governed by (A.3.3).

$$\frac{D}{Dt}\nabla^2\psi + \frac{\partial\psi}{\partial x} = U_T\left(\frac{\partial^2}{\partial y^2} - \frac{\partial^2}{\partial x^2}\right)v_- + 2U_T\frac{\partial^2 u_-}{\partial x\partial y}$$

where

$$\frac{D}{Dt} \equiv \frac{\partial}{\partial t} + \overline{U}\frac{\partial}{\partial x} \qquad \text{(A.3.3a)}$$

$$\overline{U} = \left(\overline{u_1} + \overline{u_3}\right)/2, \qquad U_T = \left(\overline{u_1} - \overline{u_3}\right)/2 \qquad \text{(A.3.3b)}$$

The baroclinic mode is governed by (A.3.4).

$$\frac{Du_-}{Dt} - yv_- + \frac{\partial\phi_-}{\partial x} = -U_T\frac{\partial u_+}{\partial x} \qquad \text{(A.3.4a)}$$

$$\frac{Dv_-}{Dt} + yu_- + \frac{\partial\phi_-}{\partial y} = -U_T\frac{\partial v_+}{\partial x} \qquad \text{(A.3.4b)}$$

$$\frac{\partial\phi_-}{\partial x} + \frac{\partial u_-}{\partial x} + \frac{\partial v_-}{\partial y} = yv_+U_T \qquad \text{(A.3.4c)}$$

The barotropic mode is essentially a Rossby wave modified by a forcing arising from the baroclinic mode acting on the vertical shear.

The baroclinic mode is governed by a modified shallow water equation including the feedback from the barotropic mode.

The forcing terms on the RHSs of Eqs. (A.3.3) and (A.3.4) indicate interactions between the barotropic and baroclinic modes in the presence of vertical shear.

How vertical wind shear Changes structure of the ERW

Coupling of baroclinic and barotropic modes in the presence of vertical she

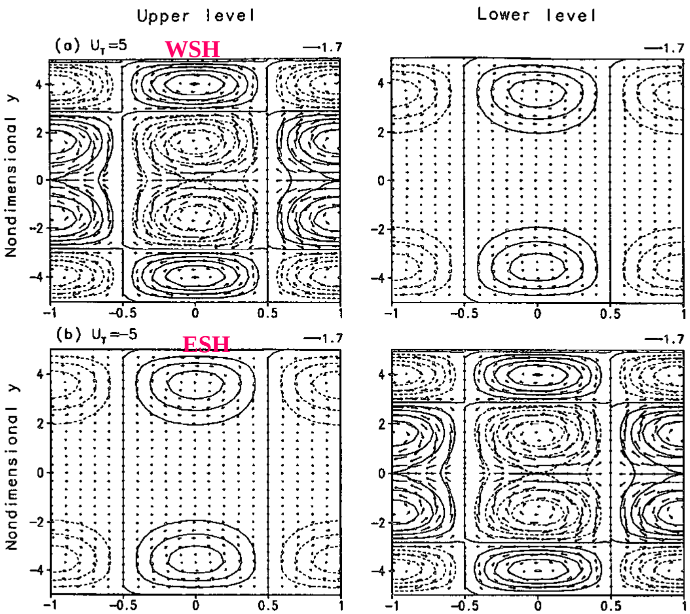

$$\frac{D\zeta_+}{Dt} = -v_+ + U_T\left(\frac{\partial D_-}{\partial y} - \frac{\partial \zeta_-}{\partial x}\right)$$

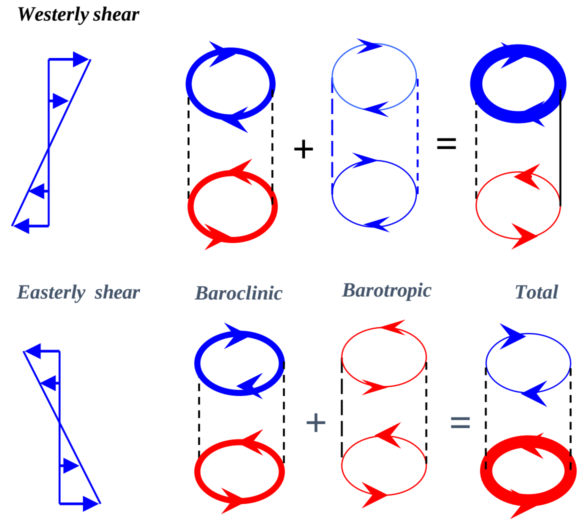

Wang and Xie (1996)

The baroclinic and barotropic modes are nearly in phase (180^{o} out of phase) in the westerly (easterly) shear. Therefore, an easterly (westerly) shear leads to the amplification of Rossby wave responses in the lower (upper) level.

Monsoon Easterly Vertical Shear can change the horizontal structure of ERW dramatically

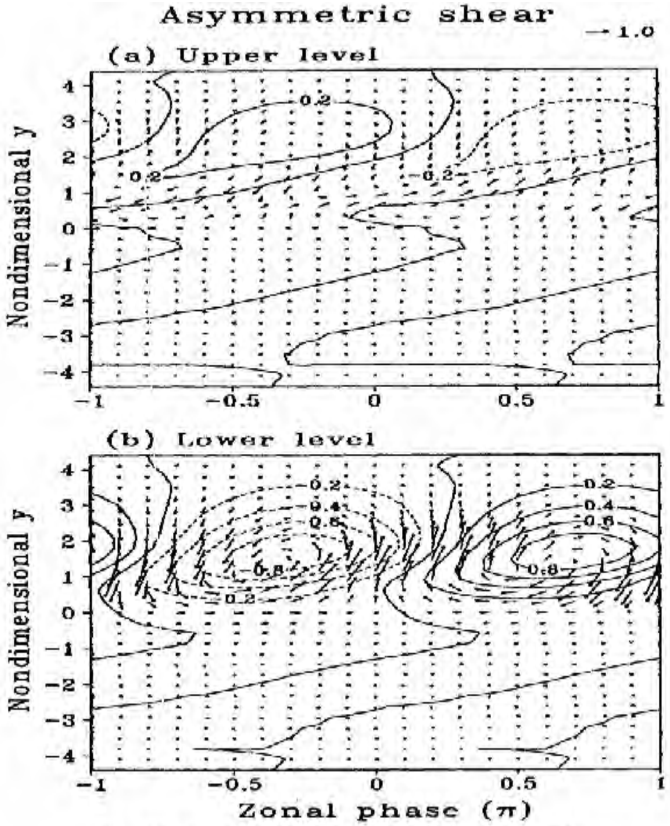

FIG. 12. (a) As in Fig. 2c, and (b) as in Fig. 2d, except for a shear of Fig. 8b.

Vertical easterly shear sets in NH only

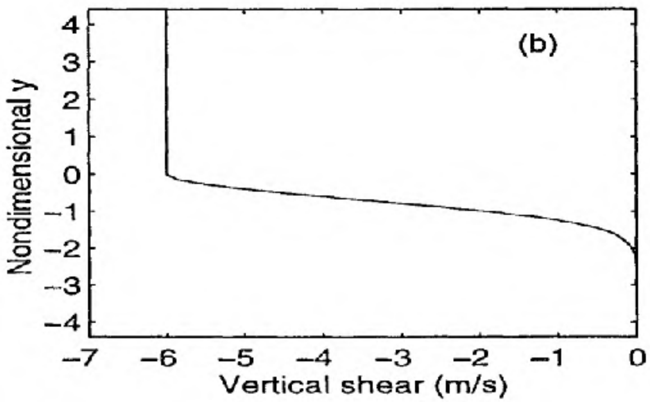

Rossby waves will be enhanced in the vicinity of the latitudes where the vertical shear is strengthened.

Model Equations on equatorial beta-plane

$$\frac{\partial u}{\partial t} - \beta y u = \frac{\partial \phi}{\partial x} + M(u) - \varepsilon u \qquad (1)$$

$$\frac{\partial v}{\partial x} + \beta y u = -\frac{\partial \phi}{\partial y} + M(v) - \varepsilon v \qquad (2)$$

$$\frac{\partial u}{\partial x} + \frac{\partial v}{\partial y} + \frac{\partial \omega}{\partial p} = 0 \qquad (3)$$

$$\frac{\partial}{\partial t}\frac{\partial \phi}{\partial p} + \bar{S}(p)\omega = -\frac{R}{C_p p} Q_c(p) + M\left(\frac{\partial \phi}{\partial p}\right) - \mu \frac{\partial \phi}{\partial p} \qquad (4)$$

$$\frac{\partial}{\partial t}\int_{p_u}^{p_s} q \frac{dp}{g} + \int_{p_u}^{p_s}\left(u\frac{\partial \bar{q}}{\partial x} + v\frac{\partial \bar{q}}{\partial y}\right)\frac{dp}{g} = -\frac{1}{L_c}\int_{p_u}^{p_s} Q_c \frac{dp}{g} + E_v + M(q) \qquad (5)$$

$$\bar{q}(p) = q_s\left(\frac{p}{p_s}\right)^{\frac{H}{H_1}-1} \qquad q_s = q_s(SST)$$

Wang 1988

Mean Flow Terms

$$M(u) = \left(-\overline{u}\,\frac{\partial u'}{\partial x} - u'\,\frac{\partial \overline{u}}{\partial x} - \overline{v}\,\frac{\partial u'}{\partial y} - v'\,\frac{\partial \overline{u}}{\partial y} - \overline{\omega}\,\frac{\partial u'}{\partial p} - \omega'\,\frac{\partial \overline{u}}{\partial p} \right)$$

$$M(v) = \left(-\overline{u}\,\frac{\partial v'}{\partial x} - u'\,\frac{\partial \overline{v}}{\partial x} - \overline{v}\,\frac{\partial v'}{\partial y} - v'\,\frac{\partial \overline{v}}{\partial y} - \overline{\omega}\,\frac{\partial v'}{\partial p} - \omega'\,\frac{\partial \overline{v}}{\partial p} \right)$$

$$M\left(\frac{\partial \phi}{\partial p}\right) = -\overline{u}\,\frac{\partial^2 \phi}{\partial x \partial p} - u'\,\frac{\partial^2 \overline{\phi}}{\partial x \partial p} - \overline{v}\,\frac{\partial^2 \phi}{\partial y \partial p} - v'\,\frac{\partial^2 \phi}{\partial y \partial p}$$

$$M(q) = -\int_{p_u}^{p_s} \left(\overline{u}\,\frac{\partial q}{\partial x} + \overline{v}\,\frac{\partial q}{\partial y} \right) \frac{dp}{g}$$

Structure of three-layer model of ISO

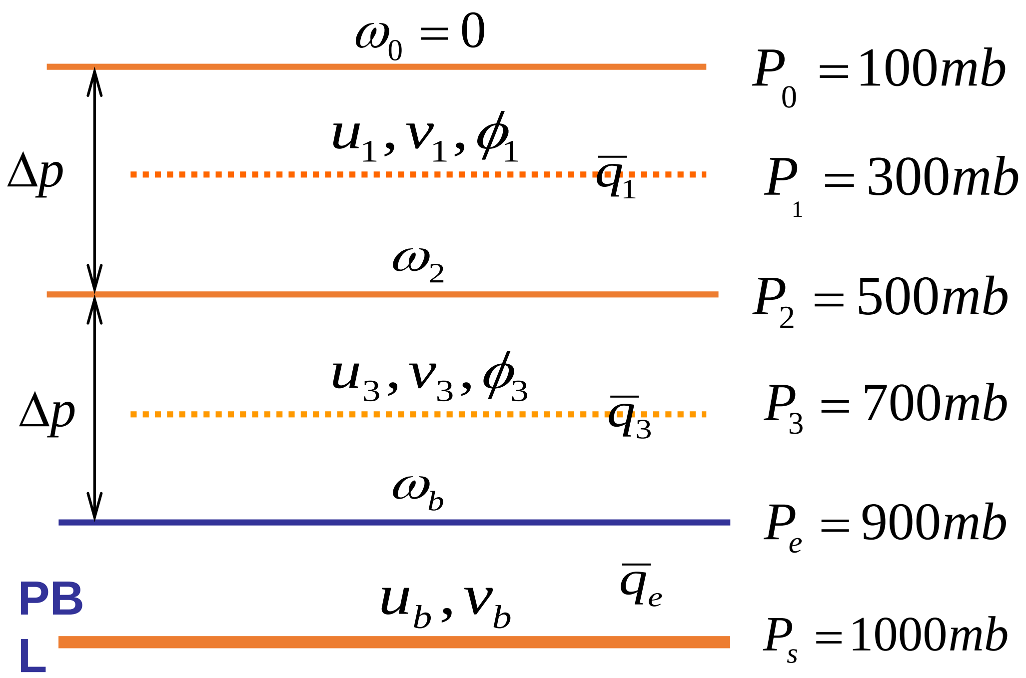

BSISO Model

The two and half layer model including

Observed Mean flows (U,V,W,T)

Realistic q_s or SST

Nonlinear heating (SST dependent trigger function and positive only heating)

Initial value problem

July mean state (ER40)

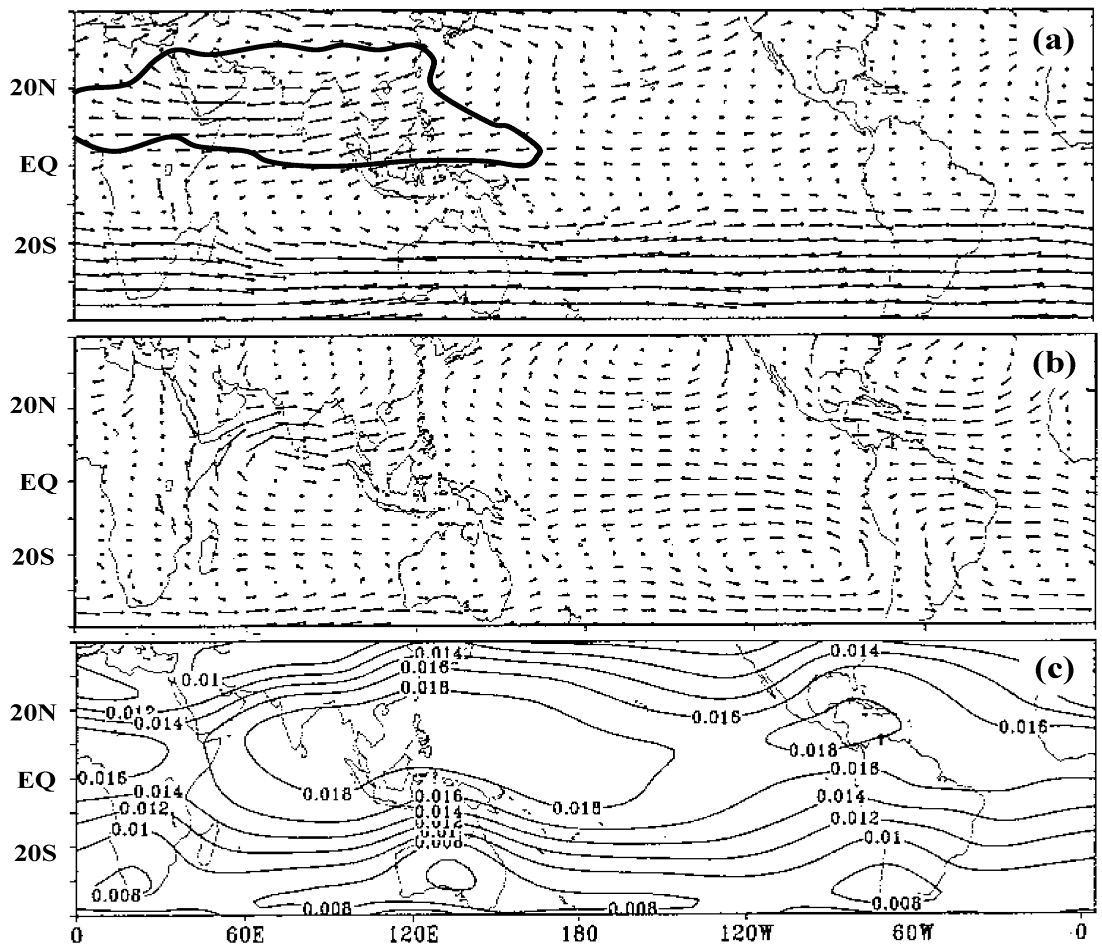

Simulated boreal summer convectively coupled Kelvin-Rossby waves

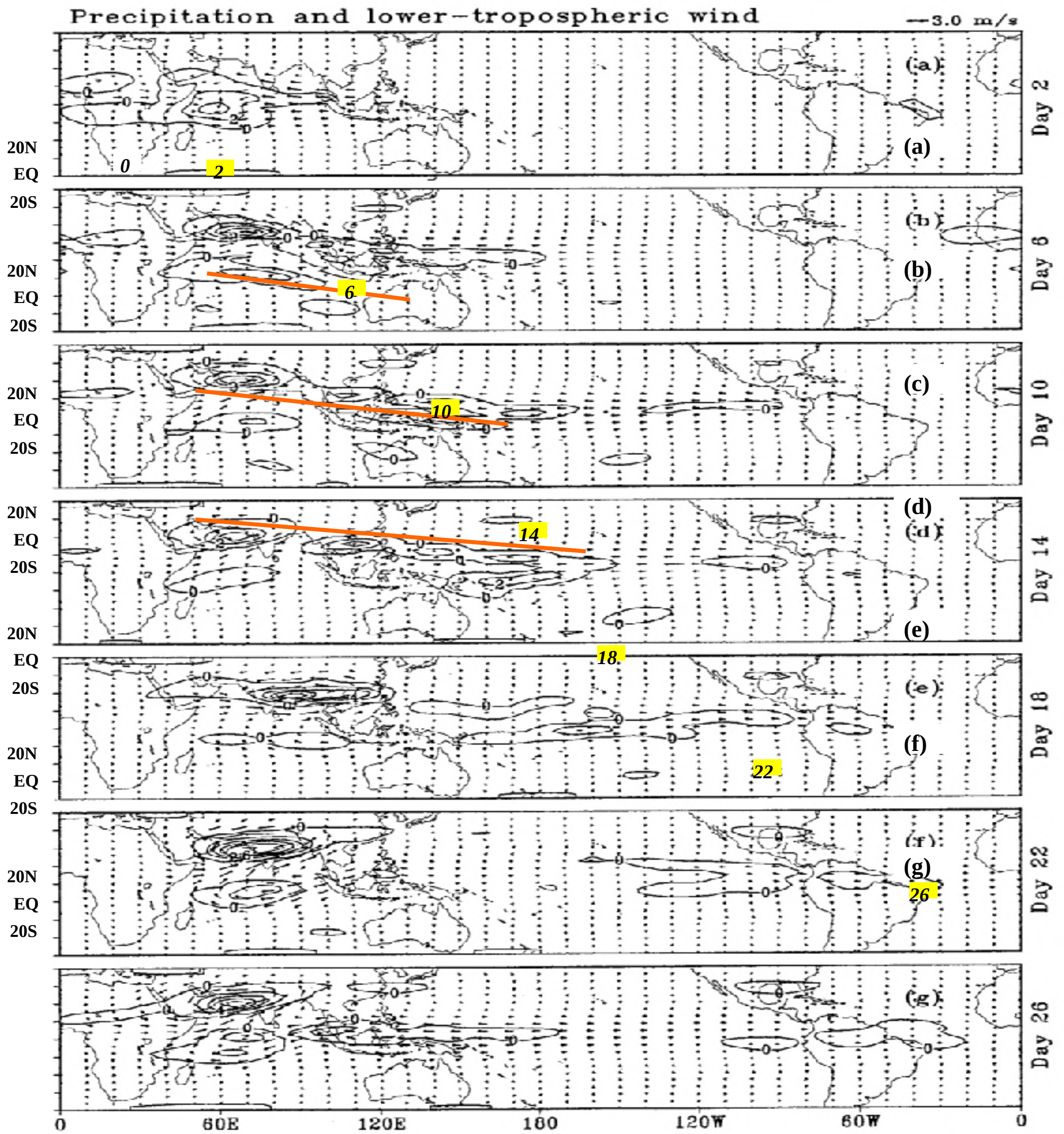

Mean flows and SST distribution trap ISO in eastern hemisphere

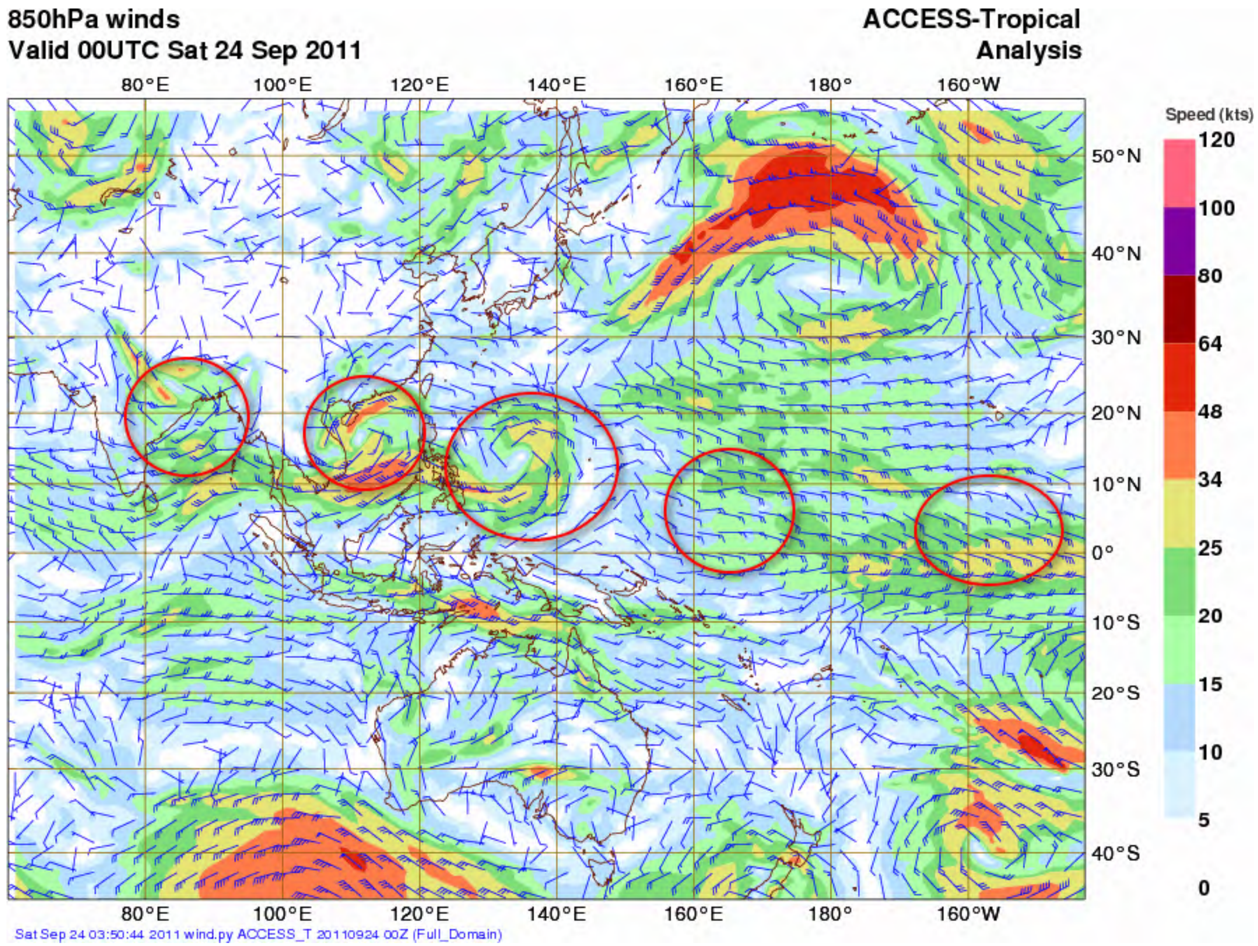

850hPa winds
Valid 00UTC Sat 24 Sep 2011
ACCESS-Tropical
Analysis
80°E
100°E
120°E
140°E
160°E
180°
160°W
50°N
40°N
30°N
20°N
10°N
0°
10°S
20°S
30°S
40°S
Speed (kts)
120
100
80
64
48
34
25
20
15
10
5
0
Sat Sep 24 03:50:44 2011 wind.py ACCESS_T 20110924 00Z (Full_Domain)

Impact on Synoptic-Scale Wave Train (SWT) in WNP

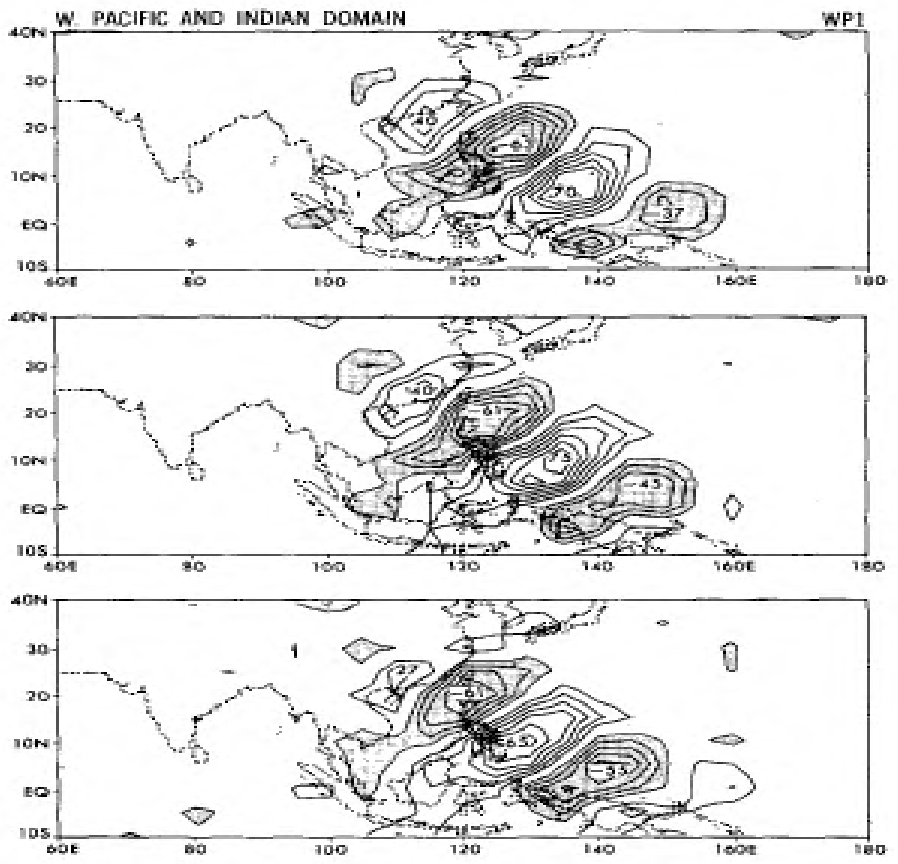

Lau and Lau (1990) :
An alternative positive and negative vorticity wave train with
timescale: 2-8 days,
wavelength: 2500 km,
propagation: northwestward.

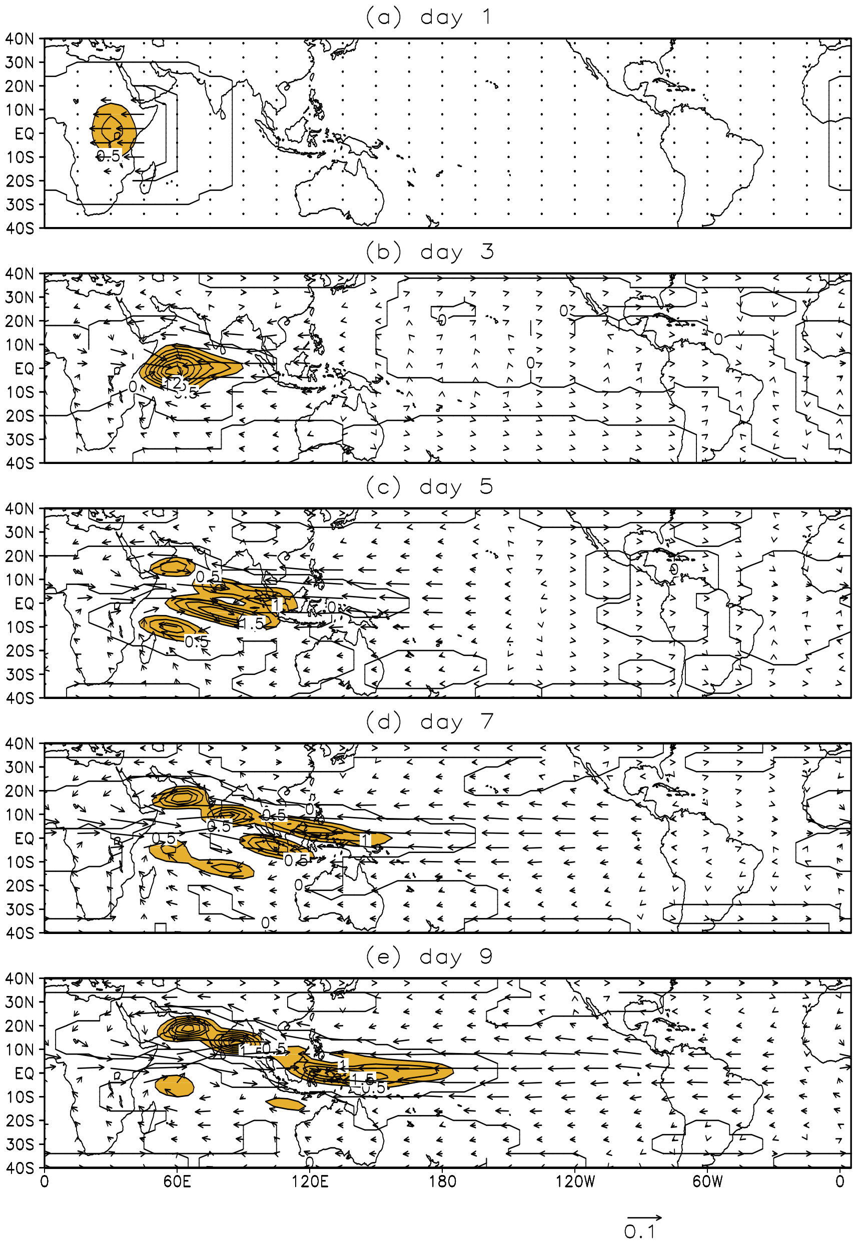

In the model, the NW-SE slanted precipitation anomalies in the monsoon regions forms due to emanation of the moist Rossby waves from the equatorial rainfall anomalies over the maritime continent.

Drbohlav and Wang 2005

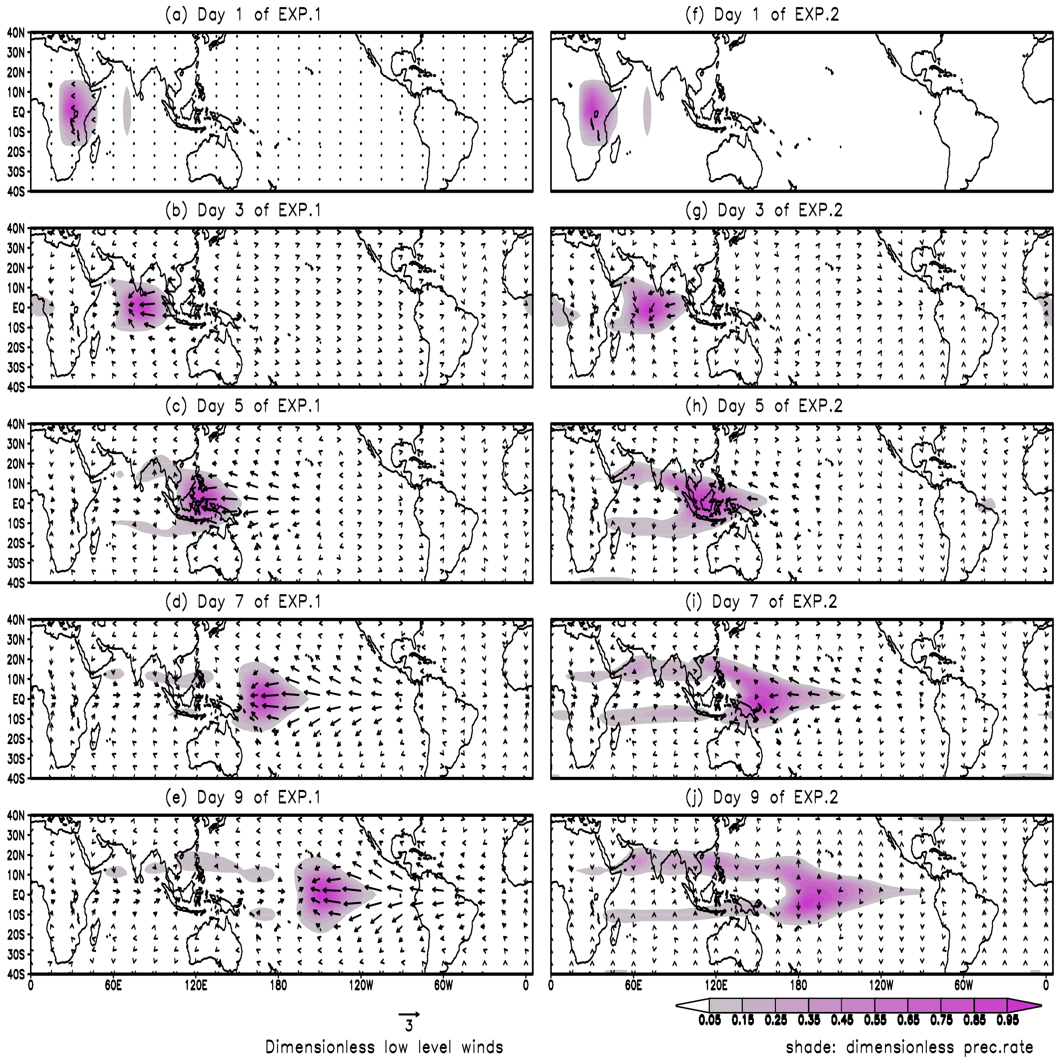

Mean flows removed
Uniform SST

Only Monsoon vertical
Shear included

Interaction between moist Rossby wave and the vertical shear of the mean monsoon provides a mechanism for the formation of the slanted ISO rain band.

Drbohlav and Wang 2005

ECHAM Model: Vorticity leads convection anomalies

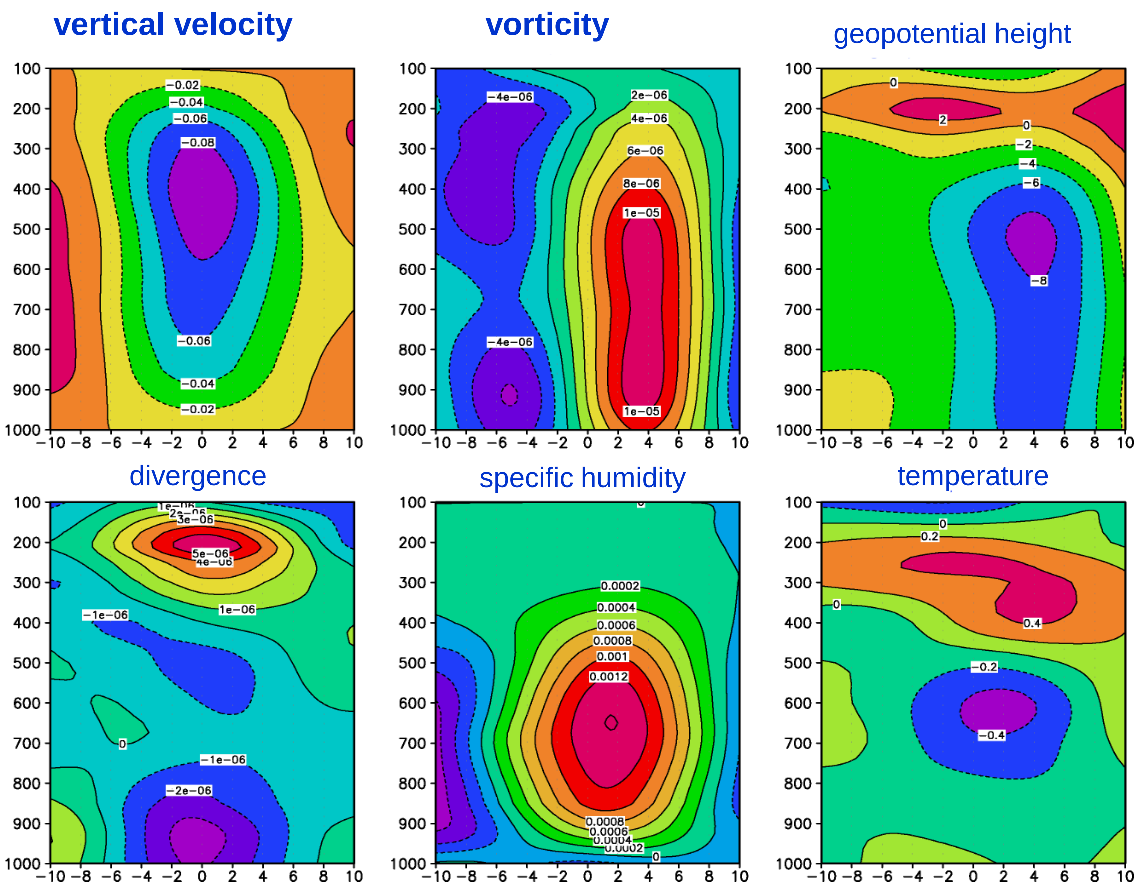

Jiang et al. 2003

How easterly vertical shear pulls the RW Northward

$$\frac{\partial \varsigma_+}{\partial t} = -\beta v_+ - U_T \left(\frac{\partial \omega}{\partial y} \right)$$

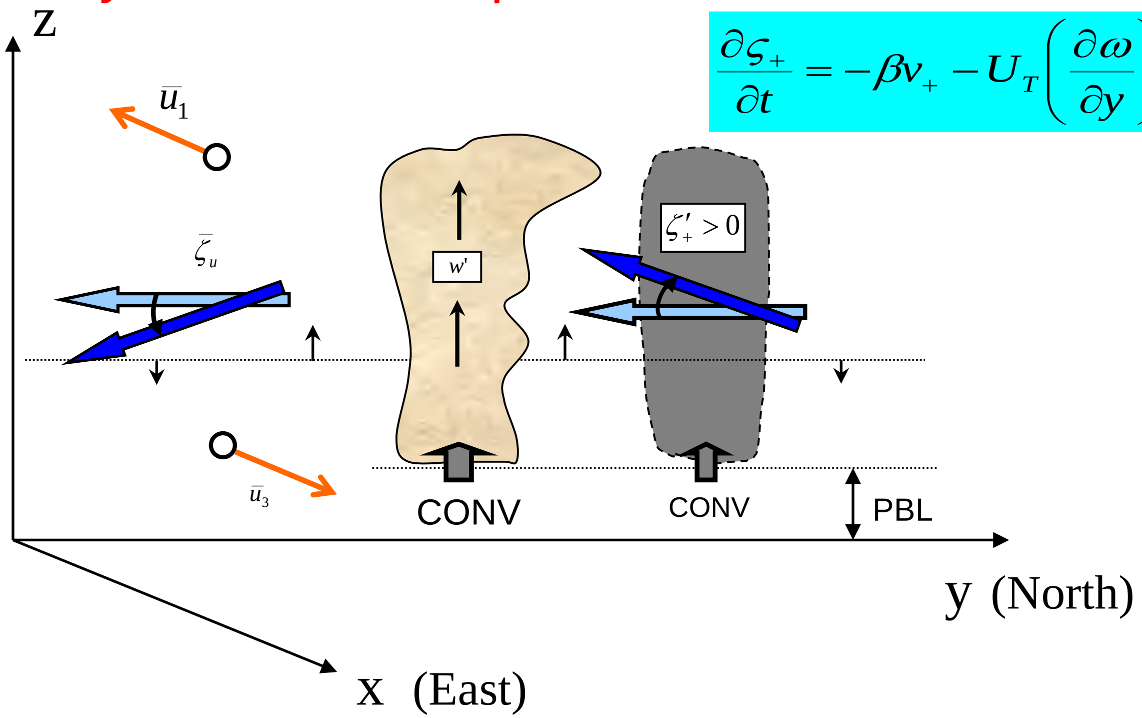

An atmospheric internal dynamic mechanism for northward propagation: monsoon easterly vertical shear provides a vorticity source, which, upon being twisted by the north-south varying vertical motion field associated with the Rossby waves, generates positive vorticity north of the convection, creating boundary layer moisture convergence that favor northward movement of the enhanced rainfall.